Received: 9 August 2018 | Accepted: 1 March 2019
DOI: 10.1002/hyp.13436

RESEARCH ARTICLE

WILEY

From on high: Geochemistry of alpine springs, Niwot Ridge, Colorado Front Range, USA

Jordan F. Fields | David P. Dethier

Department of Geosciences, Williams College, Williamstown, MA 01267

Correspondence
David P. Dethier, Department of Geosciences, Williams College, 947 Main Street, Williamstown, MA 01267.
Email: ddethier@williams.edu

Funding information
National Science Foundation; Keck Geology Consortium, Grant/Award Number: NSF EAR-1062720; NSF Boulder Creek CZO Project, Grant/Award Number: NSF-0724960

Abstract

Snowmelt-fed springs and small (0.5 km^2) upland catchments in alpine areas of the western United States contribute significantly to the quantity and inorganic chemistry of water delivered to downstream basins but have not been studied extensively. Mineral weathering, transit time, and hydrologic mixing control the solute chemistry of waters that drain the upland zone of Niwot Ridge, Colorado Front Range, and adjacent areas in the granitic core of the Southern Rocky Mountains. Water in 37 springs sampled in this study flows in generally short steep paths (~0.3 km) through shallow regolith with mean transit times (MTT) of weeks to months, producing solutions dominated by Si, Ca^{2+}, Na^+, and HCO_3^-, locally SO_4^{2-}. Rock type is a significant control on spring, surface, and shallow groundwater chemistry, and plagioclase (oligoclase) is the major source of dissolved Na^+ and Si. Concentrations of Ca^{2+} exceed stoichiometric predictions of oligoclase weathering by ~3.5×; excess Ca^{2+} likely represents weathering of aeolian material, vein calcite, or trace minerals. Concentrations of base cations and Si increase slowly with estimated MTT of 0.2 years for Niwot Ridge spring waters, and several years for shallow groundwater sampled by wells. Chemical weathering of silicate minerals is slow with estimated rates of ~2.0 and 0.2 pmol·m^{-2}·s^{-1} for oligoclase and microcline, respectively; the most mineralized spring waters are saturated only with respect to kaolinite and montmorillonite. More than 50% of the dissolved base cations + Si measured in Boulder Creek at Orodell (~25 km downstream) accumulate before water emerges from alpine springs on Niwot Ridge. Warming global temperatures are shifting more high-elevation precipitation to rain, potentially changing run-off patterns, transit time, and solute loads. Acquisition of solutes by alpine waters thus has implications far beyond small upland catchments.

KEYWORDS

alpine springs, chemical weathering, mean transit time, orthoclase

1 | INTRODUCTION

Snowmelt is an important source of high-quality water during the summer months in the western United States and in many other alpine regions, where mountains serve as "water towers to the world" (Messerli, Viviroli, & Weingartner, 2004). Ephemeral snowmelt springs, which drain the shallow subsurface and flow from the peak melt season until late summer, are relatively simple geochemical systems that contribute substantially to run-off from upland catchments. Spring chemistry records chemical weathering processes in the alpine critical zone (Baraer et al., 2015; Thorn, 1976) and provides important contributions to downstream inorganic water quality.

Most snowmelt run-off in the Southern Rocky Mountains is generated between 3,100 and 3,700 m (Segura & Pitlick, 2010), where

~80% of precipitation historically has fallen as snow (Caine, 1995), producing flow during the late spring and summer. As climate changes, however, rising mean annual temperatures will affect precipitation form and snowmelt timing in the Colorado Front Range (Clow, 2010), altering hydrologic patterns and potentially stressing downstream water resources (e.g., Musselman, Clark, Liu, Ikeda, & Rasmussen, 2017). Hydrologic changes may be significant in small alpine catchments (Zhang et al., 2018), potentially affecting the solute chemistry of run-off.

1.1 | Water chemistry and mineral weathering

Spring shallow groundwater and headwater-stream chemistry is a function of specific reaction pathways, mineral surface area, and reaction rates. Ephemeral springs may sample water draining relatively uniform geologic material, whereas headwater streams are likely to include contributions from multiple sources whose chemistry and discharge control solute levels at a point (e.g., Cowie et al., 2017; Zhang et al., 2018). Inflow of water from most source areas (e.g., bedrock, regolith, snowpack, or atmosphere) is temporally variable. Rapid snowmelt or direct precipitation, for instance, may dilute flow that is mainly derived from regolith sources (e.g., Dailey, 2016; Zeliff, 2013), and contributions from deeper groundwater are more important during low-flow periods, resulting in higher concentrations (Liu, Williams, & Caine, 2004). Along a flow path, inorganic water chemistry is controlled by (a) hydrologic flux, (b) material type, (c) transit time, and (d) the mixing of hydrologically distinct waters. Biogeochemical processes play an important role in soil chemical weathering but are less important controls on inorganic chemistry in bare-rock alpine areas than at lower elevation; we do not explicitly consider biogeochemical controls nor the role of N and P in this paper.

Silicate minerals, such as plagioclase, weather by hydrolysis to produce secondary minerals, such as kaolinite and its poorly crystalline precursors, and solutes such as Na^+, Ca^{2+}, and Si. For instance, oligoclase weathers to kaolinite.

$$\begin{aligned} &Ca_{0.27}Na_{0.73}Al_{1.27}\,Si_{2.73}O_8 + 1.27\,CO_2 \\ &\quad + 4.82\,H_2O \rightarrow 0.64\,Al_2Si_2O_5(OH)_4\ (\text{kaolinite}) + 0.27\,Ca^{2+} \\ &\quad + 0.731\,Na^+ + 1.46\,H_4SiO_4 + 1.27\,HCO_3. \end{aligned} \tag{1}$$

Mineral stability is determined by intrinsic (K_{sp}, the equilibrium solubility product and reaction kinetics) and extrinsic factors (saturation state or index; Anderson & Anderson, 2010; White & Buss, 2014). Silicate weathering reactions rarely reach equilibrium in the shallow subsurface. Solute activities and the solubility product describe the solution's saturation state (Ω; White & Buss, 2014).

$$\Omega = \text{Log}\,(\text{IAP}/K_{sp}), \tag{2}$$

where IAP is the ion activity product of the solutes and their respective stoichiometric coefficients, respectively, and K_{sp} is the solubility product at equilibrium

The saturation state of Niwot springs, shallow groundwater and headwater streams is a function of chemical weathering rates of minerals in regolith and bedrock fractures, modified by hydrologic flux. Where mineralogy is relatively simple, spring chemistry reflects mineral weathering and exchange reactions with clay-sized material (Clow & Mast, 2010), assuming biogeochemical uptake and sequestration are low or at a steady state (Cleaves, Godfrey, & Bricker, 1970; White & Buss, 2014). As a water parcel approaches saturation (Ω = 0) along a subsurface flow pathway, concentration changes decrease (Anderson & Anderson, 2010). On Niwot Ridge, fresh mineral surfaces may be relatively abundant in regolith that is regularly mixed by freeze–thaw processes, but temperatures are cool and shallow groundwater is dilute and far from saturation (Ω < 0). For example, typical Niwot Ridge spring water at near-neutral pH is undersaturated (Ω = −3.83) with respect to calcite. Mineral weathering rates can be estimated from solid-phase changes over time or by attributing solute activities to specific reactions (Ferrier, Kirchner, Riebe, & Finkel, 2010). We use the solute flux approach to estimate contemporary weathering rates (R, in $mol{\cdot}m^{-2}{\cdot}s^{-1}$) of major minerals in the field setting of Niwot Ridge (White & Buss, 2014).

$$R = \Delta M/(S \times t), \tag{3}$$

where ΔM is the solid or solute mass change due to weathering (mol), t is the reaction duration (s), and S is the total surface area (m^2).

1.2 | Transit time and chemical weathering rates

In field settings, reaction duration and surface area are aggregate properties and estimating probable values is complicated by the nature of subsurface flow in heterogeneous regolith and fractured bedrock (McDonnell et al., 2010). Water contact time with rock materials can be described as average age, or mean transit time (MTT), a metric for approximating the residence time of waters in a reservoir (Bolin & Rodhe, 1973). Kirchner (2016) demonstrated that MTT may be substantially underestimated using sine-wave fitting techniques and tracers such as delta ^{18}O, particularly in larger heterogeneous catchments, and that the young water fraction (F_{yw}, the fraction of flow <2.3 ± 0.8 months old) provides a more accurate measure of water contact time with rock materials. In the Boulder Creek basin (Colorado), Zhang et al. (2018) showed that F_{yw} generally was consistent with other estimates of contributions from mainly unreacted snowmelt along an elevational gradient. Clow, Mast, and Sickman (2018) used a decade-long record to demonstrate a close relationship between calculated MTT and F_{yw} across 11 granitic catchments in alpine and subalpine catchments of the western United States. Their work also showed a strong positive relationship between MTT and measures of chemical weathering such as concentrations of dissolved Na^+ and Si, suggesting the influence of reaction time on mineral weathering.

Mixing and snowmelt-based models successfully describe seasonal and downstream changes in stream chemistry on Niwot Ridge and adjacent areas (Cowie et al., 2017; Zhang et al., 2018). The geochemical approach we apply here, however, evaluates water chemistry using the perspective of chemical weathering processes, approximate

rates (Clow & Mast, 2010) and transit time, which may change as climate warms and snowmelt run-off decreases. We hypothesize that spring shallow groundwater and small drainage chemistry in the Niwot Ridge area can be described as a function of weathering reactions and approximate MTT. In our analysis, we use mineralogic and hydrogeologic information and estimated material properties to analyse the chemistry of weathering from extensive solute data collected by this and previous studies on Niwot Ridge and adjacent areas. Our approach also helps to provide a geochemical basis for estimating end-member chemistry values (Christophersen, Neal, Hooper, Vogt, & Andersen, 1990; Dailey, 2016; Liu et al., 2004; Zeliff, 2013; Zhang et al., 2018) required for modelling studies of run-off chemistry.

2 | SETTING

2.1 | Site description

Springs, headwater streams, and wells discussed here are located on the alpine and subalpine slopes of Niwot Ridge, west of Boulder, Colorado, USA (Figure 1), mainly above an elevation of 3,300 m. The ridge itself is a broad gently sloping area that decreases in elevation from >4,000 m at the Continental Divide in the west to <3,000 m 9 km to the east. For simplicity, in this paper, we refer to both the alpine and the upper subalpine zones as "alpine," recognizing that soil thickness, vegetation cover, and other biogeochemical parameters vary substantially in these zones (e.g., Lewis & Grant, 1979). Like many alpine areas in the western United States and Canada, the Niwot Ridge study area was a locus of periglacial activity above late Pleistocene glaciers that flowed in Green Lakes Valley to the south and the Lefthand drainage to the north. Niwot Ridge has a cool modern climate (mean temperature approximately −2°C near the Saddle wellfield, Figure 1), annual precipitation of ~1,000 mm, high solar radiation, extensive, patchy snow cover for much of the year, strong winds, and substantial interannual fluctuation in hydrologic processes (Caine & Thurman, 1990).

Ephemeral snowmelt-driven springs drain into small catchments (<0.5 km^2) carved into both the north and south sides of Niwot Ridge (Figure 1). Catchments on the southern side of the ridge (upper Fourmile, upper Como, Saddle, and Martinelli) empty into the Boulder Creek watershed, which drains 1,160 km^2 of the Front Range before joining St. Vrain Creek, the South Platte River and, eventually the Mississippi (Murphy, 2006). Springs on the north side of the ridge drain into Lefthand Creek, which flows into Boulder Creek near Longmont, Colorado (Murphy, 2006). With the exception of Columbine Spring and Fourmile springs, the springs sampled in this study flow for 1 to 2 months during the melt season and headwater streams flow from about May until early fall. Flow from most springs was cool (<3–4°C) and discharge rates ranged from <<1 to >4 L s^{-1} during reconnaissance sampling in 2014 and 2015, and more systematic sampling in 2016.

2.2 | Rock materials and weathering

Fractured bedrock composed primarily of Precambrian crystalline rocks and intruded by Laramide-age granitic stocks lies beneath Niwot Ridge (Cole & Braddock, 2009; Dickinson et al., 1988; Gable & Madole, 1976). Regolith 4 to >10 m thick (Leopold, Dethier, Raab, Rikert, & Caine, 2008; Madole, 1982; Major, 2015) rests on fractured lower permeability bedrock. Periglacial processes episodically sorted regolith, creating lenses and local channels composed of pebbles to

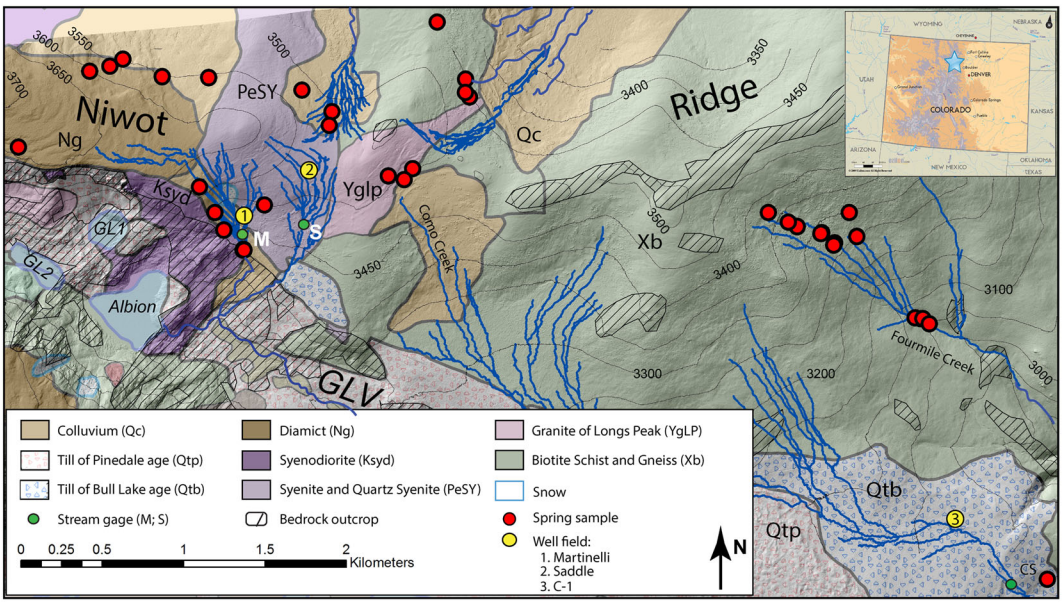

FIGURE 1 Geologic map displaying prominent surficial units, bedrock outcrops, and inferred bedrock (modified from Cole & Braddock, 2009) on Niwot Ridge as well as the location of springs sampled during this study, wells, and stream gages. Green Lake 5 and Green Lake 4 are located 2 and 1 km, respectively, west of the figure margin. CS is Columbine Spring

TABLE 1 Mineralogical data from Niwot Ridge soil and bedrock

Bedrock and soil materials[a,b,c]	Bedrock mineralogy[d]
Colluvium (Holocene and late Pleistocene; Qc)	Derived from mixed bedrock materials
Bull Lake Till (Late Pleistocene; Qtb)	Derived from mixed bedrock materials
Diamicton (Neogene; Ng)	Derived from mixed bedrock materials and from granitic bedrock and metasediments exposed to the west
Syenite and quartz syenite (Palaeocene; Pesy)	Orthoclase, plagioclase, leucite, quartz (<5%), hornblende, biotite, iron oxides (2–3% together)
Monzogabbro (Late Cretaceous; Kmzb)	Plagioclase (oligoclase–andesine), alkali feldspar, quartz (<5%), hornblende, pyroxene, sphene, and apatite (accessory)
Quartz monzonite (Late Cretaceous; Kqm)	Plagioclase (oligoclase–andesine), alkali feldspar, quartz (>10%), hornblende, lesser pyroxene, and biotite (<10% together). Light-grey porphyritic quartz-monzonite dikes with plagioclase phenocrysts throughout.
Syenodiorite (Late Cretaceous; Ksyd)	Orthoclase, quartz (5–10%), hornblende, biotite, and iron oxides (2–3%)
Monzogranite (Granite of Long's Peak); (Precambrian; Yglp)	Microcline, quartz, plagioclase, lesser amounts of muscovite and biotite, sillimanite, and garnet (trace)
Cordierite and magnetite-bearing sillimanite-biotite gneiss and metasediments (Precambrian; Xb)	Quartz, feldspar, cordierite, magnetite (4%), sillimanite, biotite,

[a]Soil nonclay minerals (weight percent by XRD, corrected for 35% peat content): quartz (28.6); total K-spar (23.8); total plagioclase (21.1); amphibole (ferrotschermakite; 1.4); haematite (0.2); goethite (0.4); maghemite (0.9); apatite (0.1). Total = 76.4.

[b]Soil clay minerals (weight percent by XRD, corrected for 35% peat content): total kaolinite (1.5); smectite + illite + muscovite (18.4); biotite (2M1; 2.4); Chlorite (CMM; 1.3). Total = 23.6.

[c]Soil data are average XRD values from 55 sites near the well field in the Saddle catchment and 4 sites in the Green Lakes Valley from Litaor (unpublished data, 2016).

[d]Bedrock classification and mineralogical data from Cole and Braddock (2009).

cobble gravel separated by more poorly sorted layers of fines, rubble derived from fractured bedrock, and aeolian material (Leopold et al., 2008). The shallow subsurface thus is vertically and laterally variable and includes buried zones of higher permeability (paleochannels) in the regolith that are the primary conduits for subsurface water in the alpine zone (Leopold, Huber, Dethier, & Weihenstephan, 2013; Leopold, Lewis, Dethier, Caine, & Williams, 2015; Williams et al., 2015) and in at least some adjacent areas (Figure 1).

The mineralogy of regolith and soils on Niwot Ridge and the adjacent Front Range mirrors underlying bedrock and is rich in plagioclase, quartz, and potassium feldspar (Kspar; Birkeland, Shroba, Burns, Price, & Tonkin, 2003). Major rock types on Niwot Ridge and adjacent areas (Figure 1) are (a) cordierite and magnetite-bearing sillimanite-biotite gneiss (Xb; shown as "gneiss" in other figures); (b) Granite of Long's Peak (Yglp); (c) quartz syenite and syenodiorite (PeSY and Ksyd); and (d) surficial deposits composed of an early Pleistocene (?) diamicton, gravelly periglacial deposits and colluvium and, on lower slopes, 130 kyr old till (Ng, Qc, and Qtb, respectively). Other bedrock types listed in Table 1 have minimal exposure in the study area. The sillimanite-biotite gneiss and granite, two of the most widespread units on Niwot Ridge, are rich in sodic plagioclase, mainly oligoclase (Table 1).

Slow chemical weathering of primary regolith minerals, particularly plagioclase, and aeolian fines delivered by persistent, high winds (Benedict, 1970; Birkeland et al., 2003; Knowles et al., 2015; Litaor, 1987a; Muhs & Benedict, 2006) has produced secondary minerals and releases solutes to infiltrating water. Oligoclase, the sole source of dissolved Na^+ and a source of Si and Ca, and Kspar are important mineral components in alpine soils and bedrock. Quartz in these rocks weathers too slowly to be a significant source of Si. Mica (including biotite) and ferromagnesian minerals, calcite and pyrite, are minor to trace constituents in the rock materials of Niwot Ridge. Calcite, in particular, is readily dissolved and represents an important potential source of Ca^{2+}. M. Litaor (Tel Hai College, Upper Galilee, Israel, unpublished data, 2016, and 2018) sampled soils from 50 sites above the Saddle wells and 5 sites (a catena of summit, backslope, and toeslope) near GL-4 (Figure 1). Litaor's comprehensive soil mineralogical data (see Table 1), determined by XRD, show that silicates (quartz, Kspar, and oligoclase) dominate the coarse fraction and that clay material is rich in smectite, illite, and muscovite, with minor kaolinite. Mahaney and Fahey (1980) reported that a latest Pleistocene palaeosol on Niwot Ridge contained abundant kaolinite.

3 | METHODS

3.1 | Field sampling

We report data from a reconnaissance study of Niwot Ridge springs in 2016 (Table A1) and in our analysis use research results (e.g., Zeliff, 2013; Dailey, 2016; Cowie et al., 2017) and the extensive database of groundwater and alpine stream chemistry and flow from Niwot Ridge and nearby areas (see Zhang et al., 2018) curated by the LTER Program (http://niwot.colorado.edu/data). We searched for and mapped springs using topographic features and late-lying snowfields and measured temperature and discharge as we collected water samples at selected springs identified in previous studies (e.g., Corona, 2013; Nesbitt & Dethier, 2013). We attempted to collect samples representative of each catchment and bedrock type. Samples were filtered through a

0.45 μm Millipore nitrocellulose membrane filter within 12 hr and stored in the dark at 4°C until analysis but were not acidified.

To expand our analyses spatially and temporally, we also plotted surface-water chemistry from downstream sites (McCleskey, Writer, & Murphy, 2012; Murphy, Shelley, Stout, & Mead, 2003) in the Boulder Creek catchment.

3.2 | Cosmogenic ^{22}Na

In addition to collecting water samples, to trace solute and water movement, we used an ion-exchange ("resin-bag") technique developed by Kaste, Lauer, Spaetzel, and Goydan (2016) to measure the concentration of ^{22}Na, a cosmogenic isotope, over a period of 5 days at six sites. Cosmogenic ^{22}Na ($t_{1/2}$ = 2.60 years) forms naturally in the atmosphere, and its concentration in streamflow provides an estimate of how long water has been out of contact with the surface, making it a potentially useful tracer on timescales of ~1 to 20 years (Kaste et al., 2016). The concentration of ^{22}Na serves as a potential indicator of MTT; we are not aware of previous studies from snowmelt-dominated environments.

3.3 | Lab chemical methods

Lab methods included analysis of 48 filtered spring samples (4 samples collected in late May and 44 more collected over 3 weeks in July 2016 from 37 springs using standard atomic absorption, ion chromatography, and colorimetric techniques for pH, cations, anions, and silica in the Environmental Analysis Lab at Williams College). We determined pH and ANC using a Fisher Scientific 320 pH meter, a Radiometer-analytical TIM840 auto-titrator and double endpoint Gran titration. We measured cations (Ca^{+2}, Mg^{+2}, Na^{+}, and K^{+}) using Atomic Absorption Spectroscopy and anions (Cl^{-}, HCO_3^{-}, SO_4^{-2}, NO_3^{-}, and PO_4^{3-}) using a Metrohm 883/863 Ion Chromatograph and filtered samples. We used a Technicon Autoanalyzer II to measure NH_4^{+} and Si on all samples. Average analytical uncertainty is 0.5% to 5% (2σ) for cations, 0.5% for anions, and ~5% to 10% for Autoanalyzer measurements. Detailed descriptions of laboratory devices and protocols are given at http://web.williams.edu/weather/watershed/ChemnotesV10.pdf. Dailey (2016) describes lab protocols and measurement uncertainty for analysis of groundwater and surface-water samples at other sites on Niwot Ridge and nearby (LTER samples).

3.4 | Estimating run-off and transit time

We needed to estimate specific run-off and water contact times with rock materials in order to (a) understand the geochemical evolution of Niwot springs, surface water, and shallow groundwater sampled in wells and (b) estimate mineral weathering rates. Recent hydrochemical studies summarized by Knowles et al. (2015), Cowie et al. (2017), and Zhang et al. (2018) and research by Nel Caine (University of Colorado, unpublished data) provide an extensive dataset for estimating run-off and MTTs for source waters in the vicinity of Niwot Ridge. We calculated the amount of snowmelt based on snow depths measured in late May as well as density and contributing area for each Niwot Ridge spring, producing an upper estimate for unit run-off at each spring, assuming evapotranspiration = 0 (see Data S1).

For transit time calculations, we used topographic analysis of the lidar base (http://niwot.colorado.edu/data/geospatial), RiverTools (http://rivix.com/), and ArcMap (http://www.esri.com/arcgis/) to calculate the length and slope of shallow paths from ridge crests and upslope snowdrifts through regolith to springs (Table S1). This technique necessarily assumes that most water follows shallow relatively permeable subsurface pathways, consistent with ephemeral spring discharge. MTTs for springs were estimated using a Darcian approach, measured distances and slopes from snowdrifts, and estimates of regolith hydrologic conductivity in King (2012): 5×10^{-4} to 5×10^{-5} ms^{-1} for most materials (Table 3 ; Figure S1). Using these measurements, limits imposed by ^{22}Na data (see Table A2), and results summarized by Zeliff (2013), Dailey (2016), and Zhang et al. (2018), we estimated MTT for major Niwot Ridge springs. For surface water and wells sampled in LTER studies, we used reported "residence times" (MTT), based on deconvolution of $\delta^{18}O$ values (Cowie, 2010; Cowie et al., 2017; Zhang et al., 2018), and F_{yw} values from those data. For Martinelli and Saddle streams, we calculated F_{yw} from $\delta^{18}O$ measured in precipitation at the Saddle NADP site and on mainly weekly streamflow samples from 2001 to 2010 (Nel Caine, University of Colorado, unpublished data).

Uncertainty for MTT was determined in two ways. For transit times calculated using Darcy's law, the uncertainty for each variable was estimated conservatively—path length (±50%), slope (±25%), and hydraulic conductivity (k; ± one half order of magnitude). Estimated uncertainty values were then calculated using the error propagation algorithms described by Taylor (1997). For the waters whose transit times were calculated from deconvolution algorithms of $\delta^{18}O$ amplitudes in precipitation and surface or groundwater, we determined uncertainty for the fraction of young water (F_{yw}). Each variable —$\delta^{18}O$ amplitude in stream or groundwater and in precipitation—was assigned an uncertainty based on analytical $\delta^{18}O$ precisions summarized in Zeliff (2013) and Dailey (2016) and calculated as described above. The activity of the cosmogenic isotope ^{22}Na (this study) helps constrain transit times of water emerging from several alpine springs but was not used as the primary metric of MTT for any water samples.

3.5 | Calculating solute flux from Niwot Ridge springs and small catchments

We needed to calculate the approximate annual flux of dissolved constituents from Niwot Ridge springs and small drainages in order to evaluate their contributions to downstream water quality and to estimate silicate weathering rates in this cool, moist but unglaciated alpine setting. We took two approaches for solute flux: (a) estimating spring run-off (Section 3.4) and using measured chemistry and (b) synthesizing flux values and concentration/discharge relations from long-term stream records collected in the Green Lakes valley adjacent to Niwot Ridge (Table S2). We assumed that our measurements of spring chemistry in 2016 are representative, based on multiple measurements for

three of the springs in 2011 and 2012 (Corona, 2013), which showed SE values for Ca, Na, and Si of <30%. Uncertainty in chemical flux from Martinelli and Saddle streams (Table S3) mainly reflects interannual variations in run-off and uncertainty about catchment size.

3.6 | Calculating weathering rates and saturation indices

To estimate contemporary weathering rates based on field measurements, we used the solute mass balance approach (White & Buss, 2014), estimated solute flux and MTT values from Niwot Ridge and mineral surface areas measured in comparable alpine settings, constrained by water chemistry, mineralogy, and textural measurements from Niwot Ridge (Table S3). Stream, surface water, and groundwater chemistry also allowed us to calculate saturation indices for Niwot waters.

We estimated oligoclase and microcline weathering rates using: (a) mineral abundances from Table 1; (b) mineral surface areas (0.05–0.21 $m^2\ kg^{-1}$) determined at an alpine site with similar geology 25 km north of Niwot Ridge (Mast, Drever, & Barron, 1990; Clow & Drever, 1996; Table S3); (c) a simple model of subsurface flow and regolith thickness of 4 to 6 m (Leopold et al., 2008); (d) solute flux values from this study (Dethier & Lazarus, 2006; Williams, Barnes, & Parman, 2011; and N. Caine, unpublished data, 2016); and (e) estimated MTT, summarized below. For instance, if the net flux of Na^+ from the Como Creek catchment (Figure 1) derives solely from oligoclase weathering, the chemical weathering rate of oligoclase can be calculated as

$$R_{wo} = \frac{C_{Na}\ x\ Q}{(M_r\ x\ C_o\ x\ A_o)}, \tag{4}$$

where R_{wo} is the chemical weathering rate of oligoclase, in $mol{\cdot}m^{-2}{\cdot}s^{-1}$; $C_{Na} \times Q$ is the annual dissolved flux of Na^+ from the catchment, in mol s^{-1}; M_r is the regolith mass in catchment; C_o is the fraction of oligoclase in the regolith; and A_o is the specific surface area of oligoclase, in m^2.

Use of K^+ and Kspar chemical weathering provides analogous results.

To calculate the saturation state of Niwot springs and groundwater samples for a suite of primary and secondary minerals, we used Aqion hydrochemistry (http://www.aqion.de/, Version 6.6.7), water analysis tools based on the USGS PhreeqC software (Parkhurst & Appelo, 2013) as a numerical solver.

3.7 | Analysing uncertainty for mineral weathering rates

We determined uncertainties for the variables included in our mineral weathering rate calculations using published analytical precisions where possible and by data analysis and estimation. For example, solute flux is a product of solute concentration (measured value for springs; mean value for small drainages), yearly run-off, and catchment area and the uncertainty associated with each variable. Uncertainties were then transferred through our weathering rate calculations (q) using standard error propagation methods outlined by Taylor (1997) and used by Graham, Verseveld, Barnard, and McDonnell (2010). The uncertainty of each variable x_n can be defined as δx_n and related to q as

$$\delta q = \sqrt{\sum_{n=1}^{N}\left(\frac{\partial q}{\partial x_n}\delta x_n\right)^2}, \tag{5}$$

where δq is the error propagated through the weathering rate calculations. Uncertainty for a variable (*W*) defined by the product of two preceding variables (*t* and *v*) is defined as

$$\delta W = \sqrt{\left(\frac{\partial W}{\partial t}\delta t\right)^2 + \left(\frac{\partial W}{\partial v}\delta v\right)^2}. \tag{6}$$

δW is then carried through the remaining calculations and combined with additional uncertainties subsequently introduced in the weathering rate calculations.

4 | RESULTS

4.1 | Summary of spring and shallow-groundwater chemistry

Samples collected from springs, shallow groundwater in wells, and small drainages on Niwot Ridge mainly were dilute solutions containing a dissolved solute load of ~450 ± 170 μmol L^{-1} at near neutral pH (mean 6.9) and showed Si > Ca^{2+} > Na^+ >> Mg^{2+} > K^+ (Table 2; Table A1). For anions, HCO_3^- >> SO_4^{2-} > Cl^- >> F^- in most samples; NO_3^- was not present in all samples but was a significant solute in some spring waters; PO_4^{-4} and NH_4^+ were present in only a few samples as minor constituents. Silica constituted a significant proportion of the dissolved load in most samples. Concentrations and the range of Cl^- values were small, suggesting minor contamination from sample collection, filtration, and analytical procedures. Shallow groundwater chemistry sampled in most wells (Cowie et al., 2017; Dailey, 2016; and Zeliff, 2013) and surface-water samples from upland catchments were broadly similar to spring chemistry, with several notable exceptions (Table 2). High concentrations of Ca^{2+} were measured in the D1 and D2 wells in the Saddle well field (Figure 1) during the driest times of the year. The highest concentrations of Ca^{2+} (4,666 μmol L^{-1}) and SO_4^{2-} (2,397 μmol L^{-1}) in D1 were an order of magnitude greater than in any other Niwot water, including the deep well at C-1 (140.65 and 37.7 μmol L^{-1}, respectively). D1 was drilled through surficial materials into fractured bedrock, interpreted as the Granite of Long's Peak (King, 2012). Water seeping from fractures in the GL-4 adit (near GL-4) and low-flow chemistry in a spring draining the rock glacier near Green Lake 5 (GL5RG) also were enriched in Ca^{2+} and SO_4^{2-}. Fresh fracture coatings in the adit consist of gypsum and silica. Alkalinity and Si values were low in the rock glacier spring and relatively high in the GL-4 adit. In general, concentrations of Ca^{2+} in springs, groundwater, and surface water were high relative to the

TABLE 2 Summary chemistry for spring samples collected on Niwot Ridge in 2016 and for surface and groundwater samples from nearby areas

		Ca	Na	Mg	K	NH_4	HCO_3	F	Cl	NO_3	PO_4	SO_4	Si
Dissolved constituent	**Value**	**μmol L^{-1}**											
Niwot Ridge Springs[a]	Minimum	5.88	3.57	1.03	2.61	0.00	29.02	0.00	9.80	0.00	0.00	5.86	0.69
	Maximum	166.22	127.39	78.85	22.46	2.33	303.28	24.58	19.20	31.06	12.40	101.26	390.46
	Mean	63.15	56.56	15.28	7.10	0.38	101.38	10.84	12.50	9.49	1.76	27.43	117.12
	Median	58.29	47.87	12.26	5.86	0.00	100.82	10.42	11.87	10.02	0.00	16.64	102.43
	Std dev	34.24	26.63	11.25	4.25	0.63	46.64	3.09	2.35	8.98	4.25	23.47	61.02
Saddle well D1[b]	Minimum	1,294.60	178.00	74.70	36.00	0.14	1,767.00	na	6.10	0.40	na	585.00	177.00
	Maximum	4,567.61	536.00	253.00	77.00	20.00	3,319.00	na	88.00	58.00	na	3,934.00	256.00
	Mean	2,751.39	289.59	289.59	48.04	3.79	2,602.83	na	20.37	10.06	na	2,003.50	201.96
	Median	2,473.96	269.35	269.35	46.16	1.37	2,705.33	na	13.54	7.19	na	1,440.60	202.40
	Std dev	1,223.92	83.41	83.41	10.05	5.75	446.30	na	23.31	12.67	na	1,168.78	17.36
C1 well SW-2[b]	Minimum	92.84	131.36	46.42	9.39	0.24	72.01	na	6.23	0.66	na	17.74	282.51
	Maximum	161.21	212.51	80.60	45.05	27.59	622.47	na	30.46	5.95	na	29.13	391.29
	Mean	144.45	168.22	72.23	18.40	2.51	536.90	na	9.62	3.74	na	19.45	361.63
	Median	144.93	165.50	72.47	16.83	1.43	538.45	na	8.29	3.92	na	18.88	359.74
	Std dev	8.51	11.74	4.25	5.64	4.04	61.29	na	3.95	1.20	na	1.90	15.45
GL-4 adit	7.17.09	954.00	147.50	140.00	74.40	0.80	915.00	na	23.40	na	na	3500.00	290.00
GL-5 RG spring[c]	Max. values	2,402.00	107.00	588.00	124.00	8.40	52.80	na	16.40	64.20	na	3,065.00	94.00
Saddle stream 1999–2011	Minimum	24.70	6.87	6.79	2.48	0.26	75.10	na	0.34	0.00	na	2.96	9.37
	Maximum	125.75	70.47	35.00	108.90	40.60	373.00	na	33.48	40.38	na	26.51	155.32
	Mean	55.77	41.07	11.43	11.56	2.77	143.36	na	3.80	3.65	na	12.68	94.27
	Median	55.52	41.17	10.69	4.65	0.99	140.93	na	1.75	2.19	na	12.75	100.91
	Std dev	14.49	14.50	4.12	16.58	5.62	41.23	na	5.83	6.05	na	3.01	37.36
Martinelli Str. 1984–2011	Minimum	8.73	4.44	0.99	0.26	0.00	1.05	na	0.28	1.00	na	0.27	0.93
	Maximum	107.79	47.42	15.02	32.88	69.40	135.40	na	38.73	88.09	na	43.30	73.81
	Mean	31.02	19.57	5.29	4.53	2.91	69.38	na	3.17	13.73	na	9.51	33.93
	Median	30.19	19.66	4.94	2.99	0.89	67.94	na	2.14	9.27	na	8.92	34.55
	Std dev	9.88	6.10	1.73	4.37	7.61	22.34	na	3.43	12.44	na	4.53	17.49
Martinelli deep well 2013 (n = 36)	Minimum	13.34	22.17	2.34	1.20	0.00	78.52	na	1.44	2.03	na	3.30	47.39
	Maximum	48.34	75.38	5.40	12.52	3.16	212.38	na	18.62	24.16	na	7.80	97.29
	Mean	30.07	38.71	3.94	4.25	1.22	136.00	na	4.62	11.75	na	5.55	74.80
	Median	30.39	38.52	3.99	3.55	0.91	131.87	na	3.75	11.45	na	6.09	79.16
	Std dev	8.64	11.31	0.82	2.62	0.76	37.53	na	3.64	5.17	na	1.15	15.45
Saddle deep wells W3, W4 2011–2013 (n = 106_151)	Minimum	19.13	51.06	2.45	2.48	0.14	106.19	na	1.78	0.65	na	3.43	133.54
	Maximum	121.59	112.42	22.32	22.87	7.27	555.76	na	29.14	15.68	na	22.00	259.00
	Mean	48.20	78.31	7.44	9.16	1.62	245.42	na	5.37	7.85	na	10.75	201.90
	Median	57.31	76.69	8.51	9.59	1.24	291.40	na	4.06	7.77	na	11.71	201.62
	Std dev	19.41	9.72	3.86	4.27	1.30	83.35	na	4.11	3.15	na	4.55	17.20

[a]This study (n = 47). na, no analysis reported. One sample from a spring-fed warm pond is not included because sulfate and phosphate levels were anomalously high, suggesting contamination.

[b]Sampled from 2011 to 2014.

[c]Sampled from 1998 to 2014 (N. Caine, unpublished data, 2016).

stoichiometric prediction of oligoclase weathering. We focus primarily on Si, the base cations, and SO_4^{2-}, inorganic constituents that mainly reflect mineral weathering.

4.2 | Material composition and spring chemistry

In headwater areas, water chemistry records reactions with geologic materials and reaction time. We classified springs by their underlying material type, using mapping summarized by Cole and Braddock (2009). We based our analysis on five major groups of rock materials (Table 1 and Table A1) including two groups of surficial deposits (Surficial 1 and 2) separated using distinct Ca/Na versus Si water chemistries. On a Piper diagram, springs flowing from syenitic and granite rocks and a group of calcium- and sulfate-rich groundwaters showed the most consistent geochemical separation (Figure 2). Springs draining gneissic rocks had a wide range of intermediate chemistries that overlap with the two groups of "surficial" springs, which showed minor separation on the basis of Ca, Mg, and Na + K. Water from

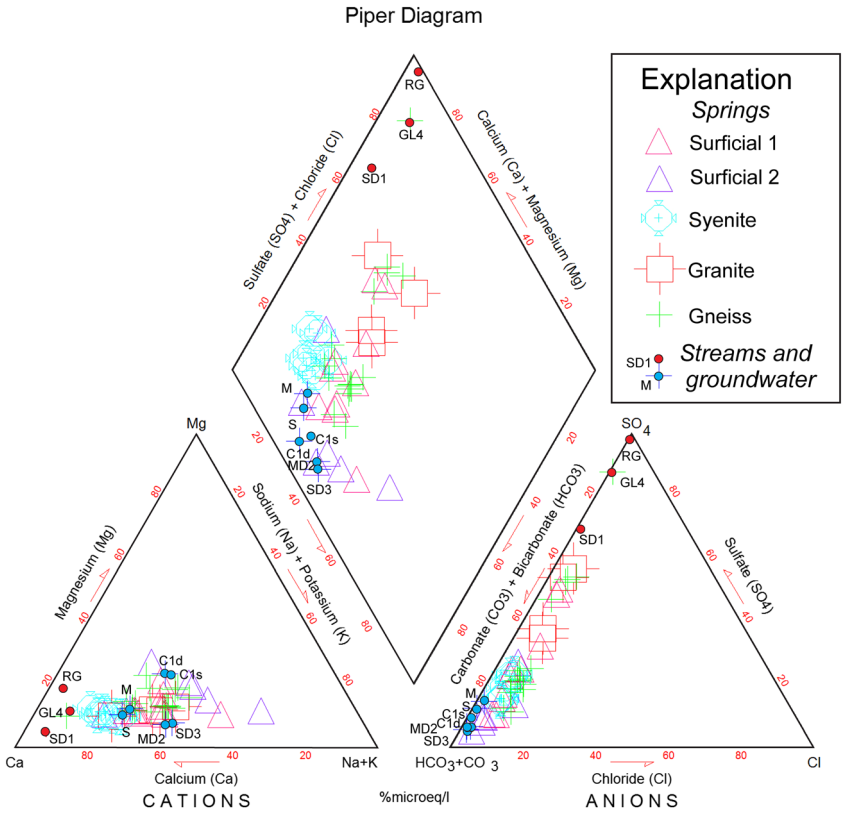

FIGURE 2 Piper diagram plotting the chemistry of Niwot Ridge springs, grouped by underlying geologic materials, and selected stream and groundwater samples. Red bullets denote high ionic strength water (SD1, Saddle well 1, deep; GL4, GL 4 adit seep; GL5RG, GL5 rock glacier spring) and blue bullets represent mainly dilute waters (C1s, C1 wellfield, shallow; C1d, C1 wellfield, deep; M, Martinelli stream; MD2, Martinelli well 2, deep; S, Saddle stream; SD3, Saddle well 3, deep)

TABLE 3 Estimated transit time and young-water fraction for waters from Niwot Ridge and adjacent areas

Water type	Years of record	Estimated mean transit time (year)					Fraction young water (F_{yw}), in %				
		Low	High	Mean	1σ	Uncertainty (±)	Low	High	Mean	1σ	Uncertainty (±)
Martinelli wells[a,b,c]	1	0.06	0.58	0.32	0.21	1.34	nd	nd	9.1	nd	nd
Niwot Ridge springs[a,c]	1	0.04	0.39	0.22	0.17	0.91	nd	nd	nd	nd	nd
Martinelli str. at gage[d]	9	0.74	1.72	1.15	nd	1.79	5.3	20	13.1	1.06	8.62
Saddle str. at gage[d]	9	0.94	3.07	1.67	nd	1.8	6.4	16	8.97	3.29	8.57
Saddle wells[b]	2	1.6	6.2	3.1	nd	nd	0.9	3.5	2	0.74	nd
Fourmile springs[a,c]	1	1.16	2.74	1.94	0.07	7.24	nd	nd	nd	nd	nd
Columbine Spring[e]	1	1.58	15.79	8.68	nd	43.02	nd	nd	nd	nd	nd
Como Cr. at weir[c,f]	13	0.77	1.83	1.13	0.36	1.83	9	18	9.02	2.45	8.33
C-1 shallow groundwater[f]	4	2.08	5.56	2.98	1.09	1.81	2.9	6	4.88	1.42	8.45
C-1 deep groundwater[f]	4	5.83	8.01	6.63	0.73	2.78	2.1	2.6	2.42	0.23	5.55

[a]nd, not determined. Calculated using Darcy's law; Niwot Ridge springs do not include Fourmile springs and Columbine Spring.

[b] F_{yw} from Zeliff (2013; table 2.4): Martinelli shallow and deep wells (2010); Saddle wells SD1-SD4, 2010 and 2011. Zeliff assumes an exponential travel time distribution and a shape factor (α) of 1.

[c]^{22}Na activity (Table A1) limits transit times. Estimated average transit time is 2–3 years for the longest travelled water (J. Kaste, written communication, 2017).

[d]Calculated from unpublished data of N. Caine (University of Colorado) for 2002–2010 assuming an exponential travel time distribution and a shape factor (α) of 1.

[e]Uncertainty in *K* value assumed to be the same as the Niwot Ridge springs.

[f]From Dailey (2016); see also Zhang et al. (2018); values assume an exponential travel time distribution and a shape factor (a) of 1.

Martinelli stream fell near the syenitic grouping, but most other stream and groundwater sample groups resemble springs draining gneiss or mixed surficial deposits rather than granite or syenite.

In springs draining the five major material types, $Si/(Ca^{2+} + Na^{+}) < 1$ in most samples and concentrations of Ca^{2+}, Na^{+}, K^{+}, and SO_4^{2-} and the Ca/Na ratio generally increased as Si increased. The strength of

the correlations and regression line slopes and intercepts varied across rock types and solutes; Na^+ correlations with Si were the most consistent with r^2 values >.4 and p < .1 except in waters that drain syenitic rocks, where there was no correlation.

4.3 | Flow path length, fraction of young water and MTT for springs, upland drainages, and groundwater in the vicinity of Niwot Ridge

Most spring waters flowed short distances (<0.3 km) on steep slopes through coarse regolith that has relatively high hydraulic conductivity, producing short calculated MTT, consistent with the ephemeral flow in the springs (Table 3; Table A2) and snowmelt-rich flow in the small alpine catchments. Columbine Spring (Figure 1), which serves as water supply for the University of Colorado Boulder's Mountain Research Station, has a longer and less well-defined flow path and shallow subsurface travel >1 km is likely for several springs that supply upper Fourmile Creek. We do not have young-water fraction (F_{yw}) data for Niwot springs, but published data for the Niwot Ridge-Green Lakes Valley area and values calculated for Martinelli and Saddle drainages (from unpublished data of N. Caine, 2016) give estimates for nearby sources (Figure 3). Values are broadly consistent with field observations of mainly snowmelt flow from the alpine area (GL-4 and Martinelli stream), snowmelt, and low but consistent baseflow during the winter (Como and other small drainages) and only slow changes in flow (groundwater in wells).

4.4 | Relationship of spring and Niwot Ridge water chemistry to flow path length and transit time

Increasing base cation concentrations were positively correlated with calculated flow-path length in some groups of alpine springs, but geochemical trends were inconsistent. Of all solutes, Si most consistently showed significant relationships with flow path length except in the gneissic rocks, where the concentration of solutes decreased with distance downgradient. When we included waters with longer transit times (Table 3) and probable contact times, median concentrations of Ca, Na, and Si were significantly related to the estimated MTT (p < .01) of waters from wells, springs, and headwater streams on Niwot Ridge (Figure 4). Field observations of relatively constant flow suggest that Columbine, the lowest-elevation spring, has a long MTT. The spring emerges from fractured bedrock downgradient from the C1 wells and likely is fed by that groundwater and by bed infiltration from Como Creek. Despite MTT estimated in years, the chemistry of these waters is relatively dilute.

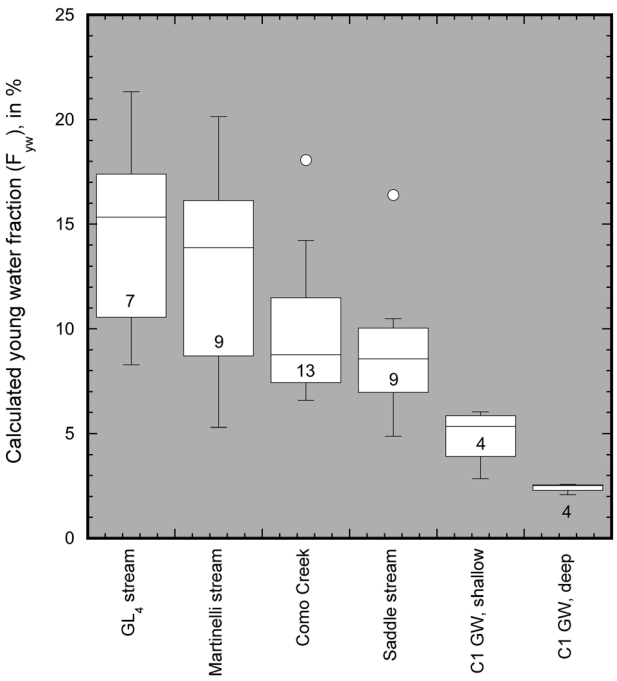

FIGURE 3 Box and whisker plot showing F_{yw} values for drainages on Niwot Ridge and in the Green Lakes Valley, compiled from δ ^{18}data in Cowie (2010), Dailey (2016), and Zhang et al. (2018). Values were not detrended, and calculations assumed that travel time distributions were exponential with a shape factor of 1. Years of record shown in (or adjacent) to bar

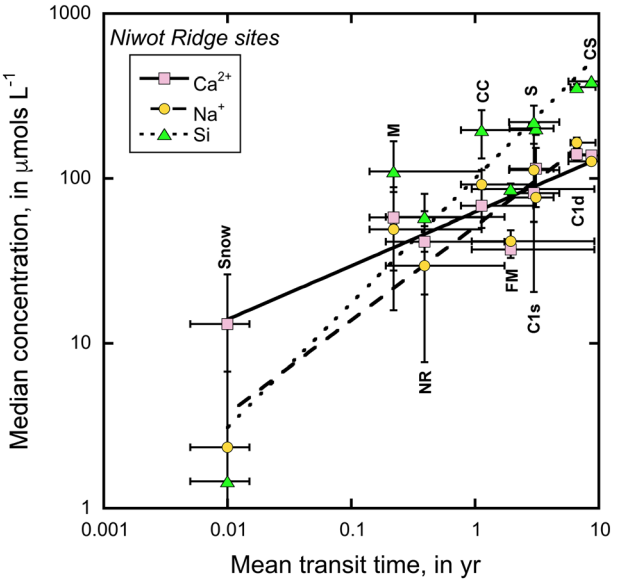

FIGURE 4 Median concentration of Ca, Na, and Si plotted as a function of mean transit time (Table 3) for water samples from Niwot Ridge. Well and Como Creek chemistry compiled by Dailey (2016). Snow, snowmelt (n = 130); NR, Niwot Ridge springs (n = 43; this study); M, Martinelli wells (n = 39); CC, Como Creek (n = 483); FM, Fourmile Springs (n = 4; this study); C1s, C1 shallow wells, (n = 565); S, Saddle wells 3, 4 (n = 152); C1d, C1 deep well, (n = 98); CS, Columbine Spring (n = 1; this study). Snow chemistry from Zeliff (2013). Ca = 62 $*t^{0.34}$; r^2 = .81; Na = 50 $*t^{0.6}$; r^2 = .76; Si = 96 $*t^{0.79}$; r^2 = .88. Error bars are shown as ± sensitivity except where the (−sensitivity value) is negative; in those cases, the 1σ value is plotted instead

4.5 | Estimated mineral weathering rates and saturation indices

Estimated solute flux (Dethier & Lazarus, 2006), combined with measurements of hillslope transit time and mineral surface area in regolith (Table S3), allowed us to use field-based data to estimate approximate weathering rates for oligoclase and microcline in the Niwot Ridge area. We held the mineral surface area constant and calculated a range of possible weathering rates using different estimates for regolith thickness and hydrologic flux (Table S3). Our results suggest weathering rates for oligoclase of ~1 to 2 pmol·m^{-2}·s^{-1} and ~0.1 to 0.4 pmol·m^{-2}·s^{-1} for microcline. Rates estimated from spring data are comparable with values estimated for headwater streams (Table 4) and similar to median values calculated by White and Buss (2014); uncertainty is substantial.

Calculated saturation indices are far from equilibrium for primary minerals in both spring and deeper groundwater samples (Figure 5); kaolinite and montmorillonite are oversaturated and amorphous silica (not shown) is at about 5% saturation in the spring samples.

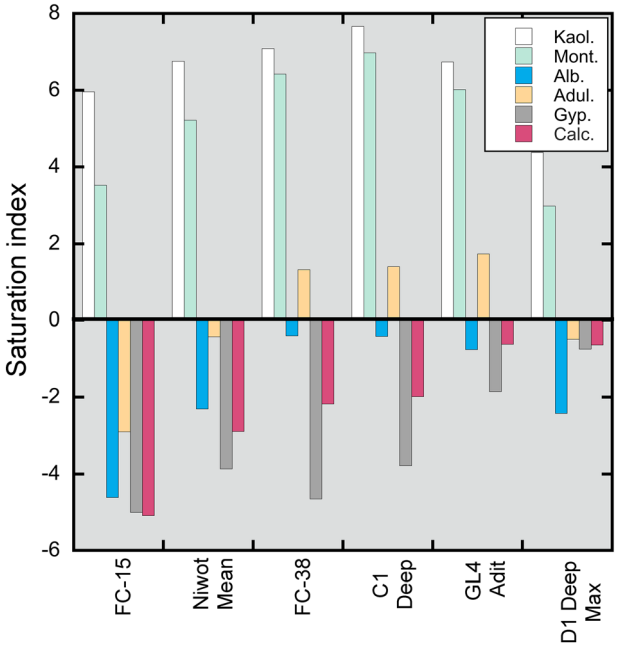

FIGURE 5 Saturation indices for major minerals in selected spring and groundwater samples from Niwot Ridge and the Green Lakes Valley (sample GL4 adit). FC-15 is typical of short-travelled springs. FC-38 is Columbine Spring. Niwot Mean is calculated from the mean concentration of Niwot Ridge springs. Kaol., kaolinite; Mont., montmorillonite; Alb., albite; Adul., adularia; Gyp., gypsum; Calc., calcite. Activity of Al^{3+} was not measured but is assumed to be 4×10^{-6} M from values in Litaor (1987b) and Litaor (2018). Indices were calculated using Aqion hydrochemistry (http://www.aqion.de/, version 6.6.7)

4.6 | Mixing and spring chemistry

Short-term changes in the chemistry of upland streams from Niwot catchments (for instance Zeliff, 2013; Knowles et al., 2015; Cowie et al., 2017) and Boulder Creek measured at a downstream site (Zhang et al., 2018) have been analysed using the mixing of different source waters. For Niwot springs, however, source area mixing does not explain significant amounts of variance in ionic content, perhaps because travel lengths are short and additions of unreacted snowmelt locally produces downgradient dilution.

5 | DISCUSSION

5.1 | Overview

On Niwot Ridge, slow plagioclase weathering exerts fundamental control on the chemistry of meltwater springs, shallow groundwater from three well fields (Martinelli, Saddle, C1) and headwater streams. Downgradient increases in dissolved constituents (from 10 to >100 μmol L^{-1}), particularly Si, record slow chemical weathering, mediated by transit time and mineral surface area. Ephemeral flow and dilute solute concentrations in most springs, shallow groundwater, and small streams suggest that they are fed by water that has a short transit time in shallow regolith. In contrast, several samples of groundwater from fractured bedrock contain solute concentrations an order of magnitude greater than values in springs. Mixing effects of such temporally and spatially variable source waters cannot be easily isolated in springs that were only sampled three times at most and are not

TABLE 4 Weathering rates calculated using spring and upland stream chemistry and estimated mineral surface area and regolith thickness on Niwot Ridge (see Table S3)

Mineral and uncertainty	Martinelli (surface water)	Saddle (surface water)	Niwot Springs[a]	White and Buss (2014) median value[b]
Oligoclase weathering rate, in pmol·m^{-2}·s^{-1}	2.14	0.91	2.41	2.00
Uncertainty (±) in pmol·m^{-2}·s^{-1}	6.75	2.63	3.05	
Microcline weathering rate, in pmol·m^{-2}·s^{-1}	0.38	0.14	0.20	1.00
Uncertainty (±), in pmol·m^{-2}·s^{-1}	0.41	0.41	0.24	

[a]Based on log-transformed chemical data.

[b]Median values from White and Buss (2014) are calculated from their Table 4.

considered in detail here. Trends in overall solute change, however, are consistent: Solute acquisition is rapid in the alpine zone and slows downstream. More than 50% of the dissolved base cations + Si measured in Boulder Creek at Orodell accumulates before water emerges from alpine springs on Niwot Ridge, some 25 km upstream.

5.2 | Solute control by chemical weathering

The geochemistry of springs, shallow groundwater, and headwater streams on Niwot Ridge reflects hydrolysis of sodic plagioclase (oligoclase), minor Kspar, and perhaps biotite, dissolution of $CaCO_3$, and at least local weathering of pyrite and calcic or ferromagnesian silicates. Sodium and Si stoichiometry in springs and groundwater closely matches ratios predicted by the weathering of oligoclase to kaolinite (Figure 6) and may reflect that primary reaction combined with release of Na^+ and Si from exchange reservoirs (Clow & Mast, 2010). Discrepancies in predicted versus observed Na^+ values (for instance Saddle D3, D4) likely reflect specific plagioclase chemistry in the syenitic rocks and minor contributions from weathering of other silicates. These data strongly suggest that the weathering of oligoclase accounts for measured concentrations of Na^+ and most of the Si in alpine waters. The concentration of Ca^{2+} and the Ca/Si ratio (Ca/Si $\approx$ 0.6; Figure 6) are too high to be explained by oligoclase weathering in all Niwot waters (Equation 1), confirming an additional non-silicate mineral source of calcium. Weathering of more calcic plagioclase would not produce Ca^{2+} or Na^+ concentrations consistent with observed values.

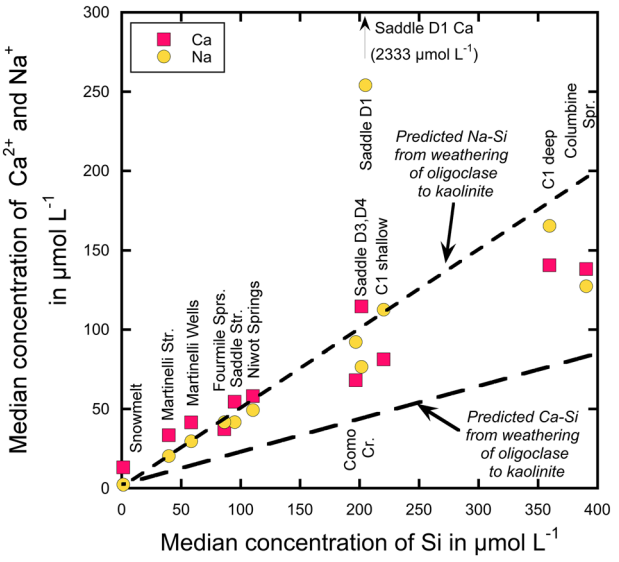

FIGURE 6 Median concentration of Ca and Na versus Si in samples of snowmelt, headwater streams, wells, and springs on Niwot Ridge. Upper dashed line plots concentrations of Na and Si predicted from the weathering of oligoclase to kaolinite. Lower dashed line plots concentrations of Ca and Si predicted from the weathering of oligoclase to kaolinite. The Ca concentration in the Saddle D1 well does not plot on this graph; arrow indicates its higher location. Well chemistry and Como Creek data from Dailey (2016). Martinelli and Saddle stream values from Caine (written communication, 2016)

"Excess" Ca is discussed widely in weathering literature (e.g., White & Buss, 2014) and has three potential sources: interstitial or vein calcite, rapid weathering of trace minerals such as pyroxene or epidote (Price, Velbel, & Patino, 2005), and calcium in dustfall (Clow, Williams, & Schuster, 2016). Calcium concentrations much greater than predicted by mineral weathering have been observed in stream waters draining similar rock types in many areas, including the Front Range 30 km north of Niwot Ridge (Clow, Mast, Bullen, & Turk, 1997). At that site, Sr isotope analysis suggested that 23% of Ca^{2+} in solution was produced by plagioclase dissolution, 26% was atmospherically derived, and nearly 50% was attributed to weathering of calcite present in trace amounts in bedrock (Clow et al., 1997, 2016). Published data do not include calcite as a Niwot Ridge mineral, but calcite and pyrite are present in mineralized veins that locally cut the bedrock. Thin calcite coatings on bedrock fractures seem unlikely as a Ca^{2+} source if groundwater has flowed through narrow fractures for millenia. However, active frost cracking in shallow bedrock and periglacial processes may act to expose fresh weathering surfaces in near-surface materials. Ferromagnesian minerals are trace constituents of rocks on Niwot Ridge, but they probably weather too slowly to be major sources of solutes in ephemeral alpine springs (Anderson & Anderson, 2010). Epidote and related Ca-silicates also are trace constituents and may be locally common in hydrothermally altered areas. Dustfall is a significant and increasing source of Ca^{2+} in some areas of the Rockies (Clow et al., 2016; Lawrence & Neff, 2009).

Field-based weathering rates estimated from spring chemistry and other hydrochemical data (Dethier & Lazarus, 2006; Litaor, 1987b; Williams et al., 2011) show that oligoclase and microcline weather slowly in the alpine zone (Table 4; Table S3). Calculated values for oligoclase fall within the broad range of field-based estimates summarized in White and Buss (2014): table 4 and fig. 20. Calculated microcline weathering rates are relatively low, suggesting that (a) Kspar is less abundant than estimates in Table 1; (b) incorporation into organic matter or secondary phases lowers values of K^+ in solution and thus calculated rates; or (c) cool temperatures depress microcline weathering rates. We do not have high confidence in our calculated rates because of uncertainties in our estimates for mineral surface area and spring hydrologic flux.

Low solubility and kinetics limit silicate weathering in the cool alpine areas of the Front Range. Spring waters are undersaturated (Figure 5) with respect to albite, gypsum, and calcite and highly oversaturated with respect to kaolinite and montmorillonite. Figure 5 *x*-axis provides a rough time scale: spring FC-15 has the shortest MTT (weeks to a few months) and C1, GL4 adit, and D1 have MTT measured in years. Silicates and vein minerals such as calcite are highly undersaturated in FC-15 but closer to saturation in the groundwater samples. If "adularia" is a close analog for potassium feldspars that are weathering on Niwot Ridge, springs with short MTT are undersaturated and other waters are near saturation or oversaturated. Kaolinite and montmorillonite are present in Niwot Ridge soils, but potassium feldspar has not been reported as a secondary phase and is not present with the gypsum and amorphous

silica that precipitate where seeps from the GL4 adit evaporate. Calculated saturation indices must be viewed as guides and approximations (Parkhurst & Appelo, 2013).

5.3 | Minor solutes

Potassium feldspar comprises ~24% of soil minerals on Niwot Ridge (Table 1), but K^+ concentrations are low in almost all shallow groundwater and surface water samples on Niwot Ridge. Low concentrations of K^+ in solution (mean of 7.1 μmol L^{-1}; Table 2) suggest that biotite weathering is insignificant in this system or that K^+ released by weathering is incorporated into secondary phases. We had hypothesized that concentrations of K^+ would be relatively high in springs draining syenitic rocks and would be strongly correlated with Si, because potassium feldspars are primarily microcline ($KAlSi_3O_8$) and perthite, which should weather to supply abundant K^+. However, these springs contained limited dissolved K^+, displayed the poorest correlation between K^+ and Si of any rock materials, and showed no relationship between Na^+ and Si. Biotite, present locally in Niwot Ridge rocks, is another potential potassium source, but uniformly low K^+ concentrations in springs, even in areas lacking vegetation, suggest that this easily weathered mineral is not an important chemical contributor.

Inferring the source of Mg^{2+} in spring waters is complicated by the uncertain origin of the high Ca^{2+} concentrations. If calcite is the source of excess of Ca^{2+} in spring waters, we would predict that Ca^{2+} and Mg^{2+} would be produced in the same molar ratio as that mineral, as is often the case in dilute, natural waters (Hem, 1985). Niwot spring samples do not confirm this hypothesis, however, and Mg^{2+} concentrations are low and variable. Variability may reflect multiple sources of Mg^{2+} including carbonate, pyroxene, and biotite (Hem, 1985). Some of the Mg^{2+} released by chemical weathering also may be sequestered in secondary phases such as smectite.

5.4 | Geochemical inferences about flow pathways from Ca^{2+}- and SO_4^{2-}-rich groundwater

High concentrations of Ca^{2+} and SO_4^{2-} at several sites in the Niwot Ridge area do not substantially influence downstream chemistry but may indicate how different flow pathways affect solute acquisition. With the exception of C1 well SW-2 (finished in till), low-flow groundwater sources (Table 2) are rich in Ca^{2+} and SO_4^{2-}. In GL5RG, Ca^{2+} and SO_4^{2-} concentrations are high but alkalinity and Si values are low; Williams, Knauf, Caine, Liu, and Verplanck (2006) attributed the unusual geochemistry at GL5RG to pyrite and epidote weathering and precipitation of silica along the flow pathway. Geochemistry of the Saddle D1 well, which is <10 m deep, suggests a simple hydrogeologic interpretation related to water level (Figure 7). When the water table is high, shallow groundwater running through surficial materials has a stable, relatively dilute chemistry. When the depth to water is >5.5 m, water is derived from fractured bedrock and Ca^{2+} (and Na^+ to a lesser degree) concentrations are high and increase with decreasing water level; Si concentrations are relatively low and alkalinity is high. Groundwater from Saddle D2 shows a similar pattern of changed molar ratios with water level, but concentrations are lower.

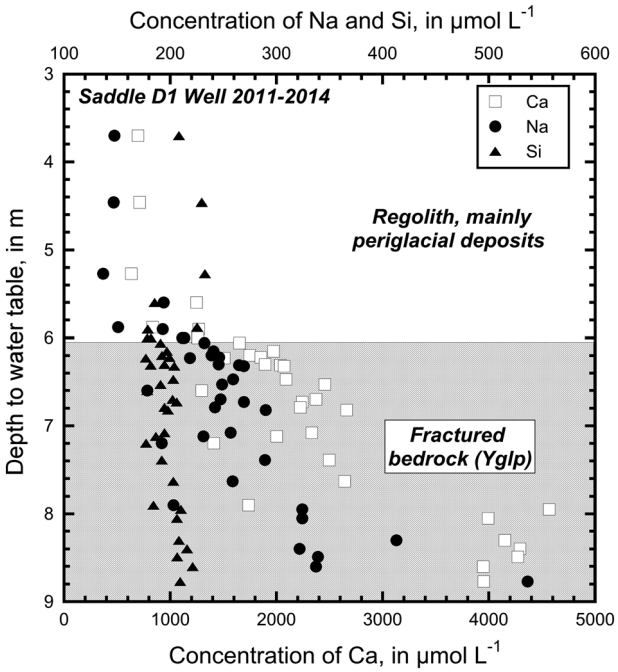

FIGURE 7 Relationship of dissolved Ca, Na, and Si to water table depth measured at the time of sampling, Saddle D1 well (data compiled by Dailey, 2016). Yglp is Granite of Long's Peak. Note: *x*-axis scales are different

Moderate transit times and chemical weathering in recently (?) fractured bedrock likely control high levels of calcium and sulfate measured in D1. Samples are nearly saturated with respect to calcite and gypsum (Figure 7) at approximately neutral pH values, suggesting concurrent pyrite oxidation and calcite dissolution. The Saddle wells were drilled in 2006, and boring may have exposed fresh bedrock and vein surfaces. The effect of pyrite oxidation is most pronounced in the two Saddle wells and at GL5RG, but pyrite, calcite, and Ca-silicate weathering may be important, local sources of SO_4 and excess Ca in other alpine waters. Solute patterns in the Saddle D1 well also suggest a model for the flow paths sampled by snowmelt springs. Water from the shallow Saddle regolith is chemically similar to the Niwot Ridge springs, indicating that the flow paths of springs from snowdrift to outflow are shallow, well-mixed, and have relatively short transit times.

5.5 | Weathering influence on solution end members

Geochemical results reported here suggest that concentrations of base cations and Si measured in springs and upland streams record the weathering of feldspar and "calcite" in the soil and shallow subsurface of Niwot Ridge. For these inorganic constituents, differences in end-member chemistry are not substantial and mainly reflect contact

time of snowmelt with regolith. Concentrations are lower where snowmelt takes short pathways through the soil and into channels and somewhat higher where streamflow is derived mainly from water that has flowed slowly through bedrock fractures. However, dustfall contributes to the solute load of melting snow, chemical weathering rates are slow in the alpine zone, and transit times are relatively short, producing groundwater chemistry that is similar to soil water. The concentrated solutions found in a few areas such as GL5RG and the D1 well in the Saddle wellfield likely represent flow from mineralized fractures and probably do not derive from the same weathering system as most upland solutes. Water sampled in the deep well at C1 and at the GL4 adit has transit times measured in years and may represent more realistic "deep" groundwater end members for upland streams on Niwot Ridge and in similar areas in the western United States.

5.6 | Alpine control of downstream geochemistry

Chemical weathering and the volume of run-off from the alpine and upper subalpine zones of Niwot Ridge and other snow-rich areas near the Continental Divide exert a strong influence on downstream chemistry in the Boulder Creek watershed. The alpine influence also may be changing as local areas of ice lenses thaw under the influence of warmer summer temperatures (Leopold et al., 2015). The median concentration of Niwot spring waters is equivalent to 56% of the dissolved load of major solutes (Ca^{2+}, Na^{+}, SO_4^{2-}, and Si) in samples 25 km downstream at the Orodell gage site (Figure 8; catchment area ~270 km^2). Lines of best fit were drawn to include median snowpack chemistry ("Snowmelt"), but Si concentrations do not change significantly from Niwot springs to 25 km downstream and Na increases only slightly, despite increasing contributions of sewage effluent downstream. Concentrations of Ca^{2+} rise downstream and there is a significant difference between the dissolved concentration at Niwot springs versus flow in Boulder Creek at Orodell. The chemostasis suggested by Na^{+} and Si concentrations implies aggregated similarity of chemical weathering pathways, transit times, and alpine snowmelt throughout the upper Boulder Creek catchment and nearby areas in the Front Range (Dethier & Lazarus, 2006; Zhang et al., 2018). Calcium may increase downstream because much of the rest of the Boulder Creek catchment is underlain by more mafic rocks and includes run-off from the Colorado Mineral Belt and associated mineralized veins. Even in the case of Ca^{2+}, >30% of the total dissolved solute concentration at Orodell is determined within the first kilometre that snowmelt travels through the watershed.

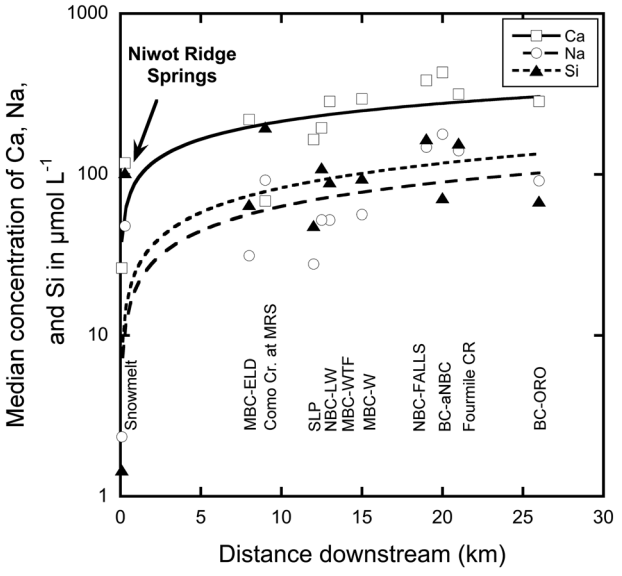

FIGURE 8 Concentration of Ca, Na, and Si as a function of approximate distance downstream from Niwot Ridge for springs and Como Creek (median values from this study and values summarized in Cowie et al., 2017) and from the Continental Divide for stream samples from throughout the upper Boulder Creek watershed (values are the mean of high-flow and low-flow concentrations from sites sampled by Murphy et al., 2003 and McCleskey et al., 2012). Sites are Middle Boulder Creek at Eldora (MBC-ELD): Como Creek at Mountain Research Station (Como Cr. at MRS); Silver Lake pipeline (SLP); North Boulder Creek near Lakewood (NBC-LW); Middle Boulder Creek west of Nederland (MBC-WTP); Middle Boulder Creek west of Barker Reservoir (MBC-W); North Boulder Creek at Boulder Falls (NBC-FALLS); Boulder Creek above confluence with North Boulder Creek (BC-aNBC); Fourmile Creek near mouth (Fourmile CR); and Boulder Creek at Orodell (BC-ORO)

6 | SUMMARY AND CONCLUSIONS

Chemical weathering of silicate-rich rocks and calcite in the alpine and upper subalpine zones controls the chemistry of water downstream in catchments draining mountainous regions such as the Colorado (USA) Front Range. Springs and streams that drain small upland catchments of Niwot Ridge are complex, dilute solutions dominated by Si, Ca^{2+}, Na^{+}, and HCO_3^{-}, locally SO_4^{2-}, which represent a mixture of snowmelt run-off, soil water, and shallow groundwater. Downstream gradients and local observations of springs and waters sampled from freshly fractured bedrock demonstrate that spring waters generally: (a) follow shallow flow paths through the subsurface; (b) have relatively short transit times; and (c) have limited contact with deep bedrock. Plagioclase weathering is the most important source of Na^{+} and Si to spring and downstream waters, but Ca^{2+} concentrations are underpredicted by silicate weathering and must have other sources, most likely the weathering of interstitial or vein calcite or aeolian material.

Solute concentrations are consistent with predictions made using field-based estimates of transit times and silicate weathering rates. However, even the most concentrated spring waters are far from saturation. In general, waters with transit times >1 year have higher concentrations and solute concentrations change incrementally as water moves downstream from subalpine and upper montane zones, joined by waters from catchments that have similar hydrogeochemistry. The alpine zone acts as an important source of water and solutes for the upper Boulder Creek watershed. Understanding how alpine

springs acquire solutes thus has implications beyond the small upland catchments of the Colorado Front Range.

ACKNOWLEDGMENTS

Field studies and measurements in the Niwot Ridge area were performed in cooperation with the NSF-sponsored NWT Long-Term Ecological Research (LTER) project. Nel Caine (University of Colorado) generously provided guidance in the field, unpublished data from the Niwot Ridge/Green Lakes area, and advice about how to interpret those data. Jim Kaste (College of William and Mary) provided materials, advice and counting for the ^{22}Na study. Iggy Litaor (Tel Hai College, Upper Galilee, Israel) shared unpublished mineralogical data from Niwot Ridge. Jason Racela (Williams College) supervised chemical analysis of the spring samples. We are grateful for the logistical help provided by personnel from the University of Colorado Mountain Research Station and by Craig Skeie, Water Resources Facility Manager, City of Boulder Watershed. Support was also provided by the NSF Boulder Creek CZO Project (NSF-0724960) and the Keck Geology Consortium (NSF EAR-1062720) and by Suzanne Anderson and Bob Anderson (University of Colorado). Detailed guidance and suggestions from two anonymous reviewers greatly improved a previous version of this paper.

ORCID

Jordan F. Fields https://orcid.org/0000-0001-7862-249X
David P. Dethier https://orcid.org/0000-0001-7501-1810

REFERENCES

Anderson, R. S., & Anderson, S. P. (2010). *Geomorphology: The mechanics and chemistry of landscapes: Cambridge* (p. 654). Cambridge: Cambridge University Press. https://doi.org/10.1017/CBO9780511794827

Baraer, M., Mckenzie, J., Mark, B. G., Gordon, R., Bury, J., Condom, T., … Fortner, S. K. (2015). Contribution of groundwater to the outflow from ungauged glacierized catchments: A multi-site study in the tropical. *Hydrological Processes*, *29*, 2561–2581. https://doi.org/10.1002/hyp.10386

Benedict, J. B. (1970). Downslope soil movement in a Colorado alpine region: Rates, processes, and climatic significance. *Arctic and Alpine Research*, *2*, 165–226.

Birkeland, P. W., Shroba, R. R., Burns, S. F., Price, A. B., & Tonkin, P. J. (2003). Integrating soils and geomorphology in mountains—An example from the Front Range of Colorado. *Geomorphology*, *55*, 329–344. https://doi.org/10.1016/S0169-555X(03)00148-X

Bolin, B., & Rodhe, H. (1973). A note on the concepts of age distribution and transit time in natural reservoirs. *Tellus*, *25*, 58–62.

Caine, N. (1995). Snowpack influences on geomorphic processes in Green Lakes Valley, Colorado Front Range. *Geographical Journal*, *161*, 55–68. https://doi.org/10.2307/3059928

Caine, N., & Thurman, E. M. (1990). Temporal and spatial variations in the solute content of an alpine stream, Colorado Front Range. *Geomorphology*, *4*, 55–72.

Christophersen, N., Neal, C., Hooper, R.P., Vogt, R.D., and Andersen, S. (1990): Journal of Hydrology, v. 116, p. 307–320.

Cleaves, E. T., Godfrey, A. E., & Bricker, O. P. (1970). Geochemical balance of a small watershed and its geomorphic implications. *Geological Society of America Bulletin*, *81*, 3015–3032. https://doi.org/10.1130/0016-7606(1970)81[3015:GBOASW]2.0.CO;2

Clow, D. W. (2010). Changes in the timing of snowmelt and streamflow in Colorado: A response to recent warming. *Journal of Climate*, *23*, 2293–2306. https://doi.org/10.1175/2009JCLI2951.1

Clow, D. W., & Drever, J. I. (1996). Weathering rates as a function of flow through an alpine soil. *Chemical Geology*, *132*, 131–141.

Clow, D. W., & Mast, M. A. (2010). Mechanisms for chemostatic behavior in catchments: Implications for CO_2 consumption by mineral weathering. *Chemical Geology*, *269*(1–2), 40–51.

Clow, D. W., Mast, M. A., Bullen, T. D., & Turk, J. T. (1997). Strontium 87/strontium 86 as a tracer of mineral weathering reactions and calcium sources in an alpine/subalpine watershed, Loch Vale, Colorado. *Water Resources Research*, *33*, 1335–1351. https://doi.org/10.1029/97WR00856

Clow, D. W., Mast, M. A., & Sickman, J. O. (2018). Linking transit times to catchment sensitivity to atmospheric deposition of acidity and nitrogen in mountains of the western United States. *Hydrological Processes*, *32*, 2456–2470. https://doi.org/10.1002/hyp.13183

Clow, D. W., Williams, M. W., & Schuster, P. F. (2016). Increasing aeolian dust deposition to snowpacks in the Rocky Mountains inferred from snowpack, wet deposition, and aerosol chemistry. *Atmospheric Environment*, *146*, 183–194. https://doi.org/10.1016/j.atmosenv.2016.06.076

Cole, J.C., & Braddock, W.A. (2009). Geologic Map of the Estes Park 30′x 60′ Quadrangle, North-Central Colorado: US Geological Survey Scientific Investigations Map 3039, v. pamphlet, p. 56 p.

Corona, C. R. (2013). Chemical response of two adjacent alpine basins in Green Lakes Valley, Colorado in a low-snow year (unpublished undergraduate thesis). Williams College, Williamstown, MA, 110 p.

Cowie, R. (2010). The hydrology of headwater catchments from the plains to the Continental Divide, Boulder Creek watershed, Colorado (MS thesis). University of Colorado, Boulder, CO, 122 p.

Cowie, R. M., Knowles, J. F., Dailey, K. R., Williams, M. W., Mills, T. J., & Molotch, N. P. (2017). Sources of streamflow along a headwater catchment elevational gradient. *Journal of Hydrology*, *549*, 163–178. https://doi.org/10.1016/j.jhydrol.2017.03.044

Dailey, K.R. (2016). Streamflow and groundwater response to precipitation variability in a snow-dominated subalpine headwater catchment, Colorado Rocky Mountains, USA (M.S. thesis). University of Colorado, Boulder, Col., 89 p.

Dethier, D. P., & Lazarus, E. D. (2006). Geomorphic inferences from regolith thickness, chemical denudation and CRN erosion rates near the glacial limit, Boulder Creek catchment and vicinity, Colorado. *Geomorphology*, *75*, 384–399.

Dickinson, W. R., Klute, M. A., Hayes, M. J., Janecke, S. U., Lundin, E. R., Mckittrick, M. A., & Olivares, M. D. (1988). Paleogeographic and paleotectonic setting of Laramide sedimentary basins in the central Rocky Mountain region. *Geological Society of America Bulletin*, *100*, 1023–1039. https://doi.org/10.1130/0016-7606(1988)100<1023:PAPSOL>2.3.CO;2

Ferrier, K. L., Kirchner, J. W., Riebe, C. S., & Finkel, R. C. (2010). Mineral-specific chemical weathering rates over millennial timescales: Measurements at Rio Icacos, Puerto Rico. *Chemical Geology*, *277*, 101–114. https://doi.org/10.1016/j.chemgeo.2010.07.013

Gable, D.J., & Madole, R.F. (1976). Geologic Map of the 7.5′ Ward Quadrangle, Boulder County, CO: U. S. Geological Survey GQ 1277, scale 1:24,000.

Graham, C. B., Verseveld, W. V., Barnard, H. R., & McDonnell, J. J. (2010). Estimating the deep seepage component of the hillslope and catchment water balance within a measurement uncertainty framework. *Hydrological Processes*, *24*, 3631–3647.

Hem, J. (1985). Study and interpretation the chemical characteristics of natural water. U. S. Geological Survey Water Supply Paper 2254, 263 p.

Kaste, J. M., Lauer, N. E., Spaetzel, A. B., & Goydan, C. (2016). Cosmogenic 22 Na as a steady-state tracer of solute transport and water age in first-order catchments. *Earth and Planetary Science Letters*, *456*, 78–86. https://doi.org/10.1016/j.epsl.2016.10.002

King, J.J. (2012). Characterization of the shallow hydrogeology with estimates of recharge at a high-altitude mountainous site, Niwot Ridge, Front Range, Colorado (MS thesis): University of Colorado, Boulder, 192 p.

Kirchner, J. (2016). Aggregation in environmental systems—Part 1: Seasonal tracer cycles quantify young water fractions, but not mean transit times, in spatially heterogeneous catchments. *Hydrology and Earth System Sciences*, *20*, 279–297.

Knowles, J. F., Harpold, A. A., Cowie, R., Zeliff, M., Barnard, H. R., Burns, S. P., … Williams, M. W. (2015). The relative contributions of alpine and subalpine ecosystems to the water balance of a mountainous, headwater catchment. *Hydrological Processes*, *29*, 4794–4808. https://doi.org/10.1002/hyp.10526

Lawrence, C. R., & Neff, J. C. (2009). The contemporary physical and chemical flux of aeolian dust: A synthesis of direct measurements of dust deposition. *Chemical Geology*, *267*, 46–63. https://doi.org/10.1016/j.chemgeo.2009.02.005

Leopold, M., Dethier, D., Raab, T., Rikert, T. C., & Caine, N. (2008). Using geophysical methods to study the shallow subsurface of a sensitive alpine. *Arctic, Antarctic, and Alpine Research*, *40*, 519–530. https://doi.org/10.1657/1523-0430(06-124)

Leopold, M., Huber, J., Dethier, D., & Weihenstephan, F. S. (2013). Subsurface architecture of the Boulder Creek Critical Zone Observatory from electrical resistivity tomography. *Earth Surface Processes and Landforms*, *1431*, 1417–1431. https://doi.org/10.1002/esp.3420

Leopold, M., Lewis, G., Dethier, D., Caine, N., & Williams, M. W. (2015). Cryosphere: Ice on Niwot Ridge and in the Green Lakes Valley, Colorado Front Range. *Plant Ecology & Diversity*, *874*, 1–14. https://doi.org/10.1080/17550874.2014.992489

Lewis, W. M., & Grant, M. C. (1979). Changes in the output of ions from a watershed as a result of the acidification of precipitation. *Ecology*, *60*(6), 1093–1097. https://doi.org/10.2307/1936955

Litaor, M. I. (1987a). The influence of eolian dust on the genesis of alpine soils in the Front Range, Colorado. *Soil Science Society of America Journal*, *51*, 141–146.

Litaor, M. I. (1987b). Aluminum chemistry: Fractionation, speciation, and mineral equilibria of soil interstitial waters of an alpine watershed, Front Range, Colorado. *Geochimica et Cosmochimica Acta*, *51*, 1285–1295. https://doi.org/10.1016/0016-7037(87)90219-5

Litaor, M. I. (2018). Soil solution chemistry in an alpine watershed, Front Range, Colorado, USA. *Arctic and Alpine Research*, *20*(4), 485–491.

Liu, F., Williams, M. W., & Caine, N. (2004). Source waters and flow paths in an alpine catchment, Colorado Front Range, United States. *Water Resources Research*, *40*, 1–16. https://doi.org/10.1029/2004WR003076

Madole, R. F. (1982). Possible origins of till-like deposits near the summit of the Front Range in north-central Colorado. U. S. Geological Survey Professional Paper 1243, 31 p.

Mahaney, W. C., & Fahey, B. D. (1980). Morphology, composition and age of a buried paleosol, Front Range, Colorado, USA. *Geoderma*, *23*, 209–218.

Major, V.W. (2015). Connecting surficial geology and hydrologic flux in leaky, snowmelt-dominated catchments, Niwot Ridge, Colorado (undergraduate thesis). Williams College, Williamstown, MA, 156 p.

Mast, M. A., Drever, J. I., & Barron, J. (1990). Chemical weathering in the Loch Vale watershed, Rocky Mountain National Park. *Water Resource Research*, *26*, 2971–2978.

McCleskey, R.B., Writer, J.H., & Murphy, S.F. (2012). Water chemistry of surface waters affected by the Fourmile Canyon wildfire, Colorado, 2010–2011. U.S. Geological Survey Open-File Report 2012–1104, 11 p.

McDonnell, J. J., McGuire, K., Aggarwal, P., Beven, K. J., Biondi, D., Destouni, G., … Wrede, S. (2010). How old is streamwater? Open questions in catchment transit time conceptualization, modelling and analysis. *Hydrological Processes*, *24*(12), 1745–1754. https://doi.org/10.1002/hyp.7796

Messerli, B., Viviroli, D., & Weingartner, R. (2004). Mountains of the world: Vulnerable water towers for the 21st century. *Ambio–A Journal of the Human Environment*, *13*, 29–34.

Muhs, D. R., & Benedict, J. B. (2006). Eolian additions to late Quaternary alpine soils, Indian Peaks Wilderness Area, Colorado Front Range. *Arctic Antarctic and Alpine Research*, *38*, 120–130. https://doi.org/10.1657/1523-0430(2006)038[0120:EATLQA]2.0.CO;2

Murphy, S.F. (2006). State of the watershed: Water quality of Boulder Creek, Colorado. U. S. Geological Survey Circular 1284, 34 p.

Murphy, S.F., Shelley, J.J., Stout, J.A., and Mead, E.P. (2003). Basic water quality in the Boulder Creek watershed, Colorado, during high-flow and low-flow conditions, 2000—Chapter 3 In: Murphy, S.F., Verplanck, P.L., and Barber, L.B., eds., *Comprehensive water quality of the Boulder Creek watershed, Colorado, during high-flow and low-flow conditions, 2000*: U.S. Geological Survey Water-Resources Investigations Report 03-4045, p. 41–70.

Musselman, K. N., Clark, M. P., Liu, C., Ikeda, K., & Rasmussen, R. (2017). Slower snowmelt in a warmer world. *Nature Climate Change*, *7*, 214–220. https://doi.org/10.1038/nclimate3225

Nesbitt, I. M., & Dethier, D. P. (2013). A comparative study of snowmelt-driven water budgets in adjacent alpine basins, Niwot Ridge, Colorado Front Range. *Geological Society of America Abstracts with Programs*, *45*(1), 101.

Parkhurst, D. L., & Appelo, C. A. J. (2013). Description of input and examples for PHREEQC version 3—A computer program for speciation, batch-reaction, one-dimensional transport, and inverse geochemical calculations. U.S. Geological Survey Techniques and Methods, book 6, chap. A43, 497 p.

Price, J. R., Velbel, M. A., & Patino, L. C. (2005). Allanite and epidote weathering at the Coweeta Hydrologic Laboratory, western North Carolina, USA. *American Mineralogist*, *90*, 101–114.

Segura, C., & Pitlick, J. (2010). Scaling frequency of channel-forming flows in snowmelt-dominated streams. *Water Resources Research*, *46*, W06524. https://doi.org/10.1029/2009WR00833

Taylor, J. R. (1997). *An introduction to error analysis* (p. 327). Sausalito, CA: University Science Books.

Thorn, C. E. (1976). Quantitative evaluation of nivation in the Colorado Front Range. *Geological Society of America Bulletin*, *87*, 1169–1178. https://doi.org/10.1130/0016-7606(1976)87<1169:QEONIT>2.0.CO;2

White, A. F., & Buss, H. L. (2014). Natural weathering rates of silicate minerals. In J. I. Drever (Ed.), *Surface and ground water, weathering and soils: Treatise on geochemistry* (2nd ed.). Amsterdam: Elsevier. https://doi.org/10.1016/B978-0-08-095975-7.00504-0

Williams, M. W., Barnes, R. T., & Parman, J. N. (2011). Stream water chemistry along an elevational gradient from the Continental Divide to the foothills of the Rocky Mountains. *Vadose Zone Journal*, *10*, 900–914. https://doi.org/10.2136/vzj2010.0131

Williams, M. W., Hood, E., Molotch, N. P., Caine, N., Cowie, R., & Liu, F. (2015). The 'teflon basin' myth: Hydrology and hydrochemistry of a seasonally snow-covered catchment. *Plant Ecology & Diversity*, *8*(5–6), 639–661. https://doi.org/10.1080/17550874.2015.1123318

Williams, M. W., Knauf, M., Caine, N., Liu, F., & Verplanck, P. L. (2006). Geochemistry and source waters of rock glacier outflow, Colorado Front Range. *Permafrost and Periglacial Processes*, *17*, 13–33. https://doi.org/10.1002/ppp.535

Zeliff, M.M. (2013). Hydrochemistry, residence time and nutrient cycling of groundwater in two, climate-sensitive, high-elevation catchments, Colorado Front Range [MS thesis]. 131 p., http://search.proquest.com/docview/1413300719?accountid=15054.

Zhang, Q., Knowles, J. F., Barnes, R. T., Cowie, R. M., Rock, N., & Williams, M. W. (2018). Surface and subsurface water contributions to streamflow from a mesoscale watershed in complex mountain terrain. *Hydrological Processes*, *32*, 954–967. https://doi.org/10.1002/hyp.11469

SUPPORTING INFORMATION

Additional supporting information may be found online in the Supporting Information section at the end of the article.

How to cite this article: Fields JF, Dethier DP. From on high: Geochemistry of alpine springs, Niwot Ridge, Colorado Front Range, USA. *Hydrological Processes*. 2019;33:1756–1774. https://doi.org/10.1002/hyp.13436

APPENDIX

TABLE A1 Location and chemical data for Niwot Ridge springs (map units noted on Figure 1)

Sample	Map unit	Rock type	Catchment/ waypoint	Date	Longitude	Latitude	Elevation (ft)	Flow path from drifts (km)	Ca^{+2} μM	Mg^{+2} μM	Na^{+} μM	K^{+} μM	NH_4^{+} μM	HCO_3^{-} μM	F^{-} μM	Cl^{-} μM	NO_3^{-} μM	PO_4^{-2} μM	SO_4^{-2} μM	SiO_2 μM
FC-1	Kysd	Syenite	Martinelli/036	7/5/16	−105.596	40.050	11,242	0.127	73.34	11.65	38.61	3.27	0.00	120.16	11.16	37.71	0.00	0.00	14.48	116.38
FC-2	Ksyd	Syenite	Martinelli/037	7/5/16	−105.596	40.050	11,199	0.127	72.22	11.07	43.87	3.76	0.00	109.84	10.63	37.31	0.00	0.00	14.28	84.50
FC-3	Kysd	Syenite	Martinelli/038	7/5/16	−105.596	40.050	11,213	0.127	73.59	11.11	49.43	4.35	0.00	114.75	10.74	37.49	0.00	0.00	14.88	92.47
FC-4	Kysd	Syenite	Martinelli/039	7/5/16	−105.597	40.051	11,317	0.02	66.17	10.33	47.87	3.50	0.00	103.28	9.74	37.80	0.00	0.00	20.58	72.55
FC-5	PeSY	Syenite	Martinelli/040/	7/5/16	−105.594	40.053	11,500	0.35	97.90	16.50	49.39	4.68	1.56	144.26	14.58	37.77	0.00	0.00	22.33	122.36
FC-6	Xb	Gneiss	Fourmile/022	7/6/16	−105.546	40.046	10,036	1.248	35.39	15.06	49.83	5.86	0.00	80.33	9.42	42.09	0.00	0.00	14.86	82.51
FC-7	Xb	Gneiss	Fourmile/020	7/6/16	−105.547	40.047	10,027	1.295	44.71	16.09	41.52	6.01	1.06	90.16	9.37	38.54	0.00	12.20	14.48	88.49
FC-8	Xb	Gneiss	Fourmile/044	7/6/16	−105.553	40.051	10,708	0.505	34.95	9.26	43.09	5.35	1.00	70.49	9.21	40.23	0.00	0.00	15.07	86.50
FC-9	Xb	Gneiss	Fourmile/045	7/6/16	−105.553	40.051	10,714	0.505	27.44	7.00	36.78	4.40	0.00	43.77	9.21	37.31	0.00	0.00	14.89	84.50
FC-10	Xb	Gneiss	Fourmile/046	7/6/16	−105.554	40.051	10,810	0.397	31.00	7.86	37.43	4.55	0.00	63.93	9.16	37.71	0.00	0.00	15.20	84.50
FC-11	Xb	Gneiss	Fourmile/047	7/6/16	−105.554	40.051	10,793	0.396	32.05	8.23	40.52	4.88	0.00	67.21	9.21	37.91	0.00	0.00	15.20	90.48
FC-12	Xb	Gneiss	Fourmile/048	7/6/16	−105.556	40.052	10,926	0.246	37.83	9.75	45.48	4.65	0.00	77.05	9.32	37.94	8.16	11.57	16.64	102.43
FC-13	Xb	Gneiss	Fourmile/049	7/6/16	−105.557	40.052	10,950	0.186	42.24	11.15	54.83	5.24	2.33	88.52	9.32	38.17	7.85	0.00	17.72	94.46
FC-14	Xb	Gneiss	Fourmile/050	7/6/16	−105.558	40.052	11,046	0.017	51.27	12.26	40.43	5.35	0.00	90.16	9.42	38.34	10.15	12.40	19.92	96.46
FC-15	Yglp	Granite	Como/033	7/6/16	−105.584	40.053	11,429	0.053	25.83	5.72	30.35	2.66	0.00	45.90	9.95	37.03	0.00	0.00	24.13	66.57
FC-16	Yglp	Granite	Como/052	7/6/16	−105.583	40.055	11,503	0.043	51.59	13.87	73.26	7.54	0.00	61.64	13.26	39.03	0.00	0.00	71.69	160.22
FC-17	Xb2	Gneiss	East Knoll/053	7/6/16	−105.580	40.060	11,330	0.057	93.76	18.44	63.78	18.01	0.00	109.84	12.68	37.91	14.35	0.00	69.46	130.33
FC-18	Xb2	Gneiss	East Knoll/054	7/6/16	−105.580	40.059	11,347	0.065	59.22	11.81	47.13	6.32	0.00	61.64	12.11	37.97	0.00	0.00	59.69	110.40
FC-19	Xb2	Gneiss	East Knoll/123	7/6/16	−105.579	40.059	11,338	0.069	56.27	11.52	57.74	6.52	0.00	56.72	16.26	42.37	8.00	0.00	64.13	128.34
FC-20	Xb2	Gneiss	East Knoll/056	7/6/16	−105.582	40.063	11,281	0.15	982.68	124.28	202.17	24.81	0.00	268.85	18.63	43.80	0.00	0.00	1156.46	168.19
FC-21	Qc	Surficial 1	N. Side Saddle/ 057	7/6/16	−105.589	40.058	11,540	0.201	58.29	11.98	76.17	3.63	0.00	116.39	10.95	40.20	10.08	0.00	27.55	128.34
FC-22	Qc	Surficial 1	N. Side Saddle/ 058	7/6/16	−105.589	40.057	11,576	0.15	97.66	19.01	77.39	9.44	0.00	153.28	11.21	37.77	16.32	0.00	33.28	154.24
FC-23	Qc	Surficial 1	Martinelli/061	7/7/16	−105.599	40.054	11,716	0.077	101.39	19.26	75.26	5.50	0.00	113.11	9.89	40.29	16.44	0.00	77.06	118.37
FC-24	Ng	Surficial 2	Green Lakes Ridge/067	7/7/16	−105.612	40.056	11,982	0.06	58.02	23.00	125.30	12.05	0.00	167.54	12.21	36.63	0.00	0.00	11.30	201.03
FC-25	Qc	Surficial 2	Martinelli/068	7/7/16	−105.598	40.052	11,453	0.03	95.15	14.77	48.13	5.14	1.22	134.43	10.42	38.06	19.35	0.00	33.71	98.45

(Continues)

TABLE A1 (Continued)

Sample	Map unit	Rock type	Catchment/ waypoint	Date	Longitude	Latitude	Elevation (ft)	Flow path from drifts (km)	Ca^{+2} μM	Mg^{+2} μM	Na^{+} μM	K^{+} μM	NH_4^{+} μM	HCO_3^{-} μM	F^{-} μM	Cl^{-} μM	NO_3^{-} μM	PO_4^{-2} μM	SO_4^{-2} μM	SiO_2 μM
FC-26	Qc	Surficial 1	N. Side of W. Knoll/069	7/8/16	−105.591	40.059	11,548	0.224	56.80	13.05	67.22	7.24	0.00	109.84	10.74	37.69	27.11	0.00	14.33	124.35
FC-27	Ng	Surficial 1	West of W. Knoll/070	7/8/16	−105.598	40.060	11,687	0.296	35.59	12.14	42.52	4.07	0.00	58.85	10.84	38.94	0.00	0.00	25.26	118.37
FC-28	Ng	Surficial 1	West of W. Knoll/071	7/8/16	−105.601	40.060	11,671	0.091	35.71	10.04	92.04	6.60	0.00	116.39	10.11	37.20	16.73	0.00	9.55	99.41
FC-29	Ng	Surficial 1	West of W. Knoll/072	7/8/16	−105.604	40.060	11,630	0.076	36.98	16.50	33.74	11.48	0.00	77.05	10.21	36.29	21.58	0.00	7.09	90.48
FC-30	Ng	Surficial 2	West of W. Knoll/073	7/8/16	−105.605	40.060	11,697	0.123	63.10	31.85	100.39	15.45	0.00	157.38	10.79	37.49	24.65	11.72	9.81	274.45
FC-31	Ng	Surficial 2	West of W. Knoll/077	7/8/16	−105.607	40.060	11,817	0.11	13.73	6.26	56.43	9.36	1.44	55.74	11.89	38.74	16.92	0.00	8.03	88.49
FC-32	Yglp	Granite	Como	7/12/16	−105.585	40.054	11,540	0.087	134.85	20.12	80.00	6.65	0.00	122.95	24.58	39.66	15.06	0.00	101.26	182.53
FC-33	Yglp	Granite	Como/033	7/17/15	−105.584	40.053	11,429	0.053	36.68	8.02	39.48	2.94	0.00	59.51	10.32	36.97	0.00	0.00	31.67	88.49
FC-34	Xb2	Gneiss	East Knoll/054	7/17/15	−105.580	40.059	11,347	0.065	73.83	15.68	54.17	10.08	0.00	74.59	12.79	39.71	0.00	0.00	70.40	126.34
FC-35	Qc	Surficial 1	N. Side Saddle/ 058	7/17/15	−105.589	40.057	11,576	0.15	92.46	18.40	74.48	9.57	1.22	152.95	11.05	38.14	17.63	0.00	29.76	145.52
FC-36	Qc	Surficial 1	N. Side West Knoll/069	7/17/15	−105.591	40.059	11,548	0.224	59.93	15.23	72.22	6.21	0.94	112.95	10.63	37.94	31.06	0.00	16.15	154.77
FC-37	Ng	Surficial 2	West of W. Knoll/073	7/17/15	−105.605	40.060	11,697	0.123	70.39	34.12	121.74	14.99	0.00	177.38	11.11	37.29	26.94	11.55	9.82	205.58
FC-38	Qtb	Surficial 2	Lower Como/ 109	7/18/16	−105.538	40.032	9,583	0.747	138.22	78.85	127.39	11.36	1.78	303.28	13.89	40.03	10.65	11.58	19.51	390.46
FC-39	Xb	Gneiss	Fourmile/050	7/18/16	−105.558	40.052	11,046	0.017	61.05	14.73	40.74	6.01	0.00	100.82	9.53	38.66	11.79	0.00	23.95	118.99
FC-40	Xb	Gneiss	Fourmile/022	7/18/16	−105.546	40.046	10,036	1.248	38.22	17.16	32.83	4.07	0.00	83.61	9.00	37.54	10.02	0.00	14.80	84.34
FC-41	Ksyd	Syenite	Martinelli/036	7/18/16	−105.596	40.050	11,242	0.127	75.41	11.07	33.91	3.32	0.00	119.67	11.37	37.34	12.82	0.00	15.07	102.82
FC-42	Ksyd	Syenite	Martinelli/039	7/18/16	−105.597	40.051	11,317	0.02	70.37	11.65	32.65	2.61	1.06	101.64	9.84	37.17	14.76	0.00	22.40	77.41
FC-43	PeSY	Syenite	Martinelli/040	7/18/16	−105.594	40.053	11,500	0.35	111.66	19.34	40.39	5.04	0.72	143.77	15.05	37.57	16.71	0.00	28.13	130.54
FC-44	Qc	Surficial 1	Martinelli/061	7/18/16	−105.599	40.054	11,716	0.077	117.20	21.98	104.65	7.72	1.00	122.79	9.79	41.63	14.55	0.00	88.04	130.54
FC16-W1	Xb	Gneiss	Fourmile Spring/004	5/25/16	−105.547	40.047	10,042	1.237	36.39	14.81	42.09	13.55	0.00	80.33	8.63	62.91	7.87	0.00	8.99	97.88
FC16-W2	Xb	Gneiss	Fourmile Stream/005	5/25/16	−105.548	40.047	10,090	1.165	20.02	7.37	33.09	3.99	1.33	47.54	0.00	38.80	17.87	0.00	5.86	59.95

(Continues)

TABLE A1 (Continued)

Sample	Map unit	Rock type	Catchment/ waypoint	Date	Longitude	Latitude	Elevation (ft)	Flow path from drifts (km)	Ca^{+2} µM	Mg^{+2} µM	Na^{+} µM	K^{+} µM	NH_4^{+} µM	HCO_3^{-} µM	F^{-} µM	Cl^{-} µM	NO_3^{-} µM	PO_4^{-2} µM	SO_4^{-2} µM	SiO_2 µM
FC16-W3	Xb	Gneiss	Fourmile Snowmelt/ 007	5/25/16	−105.552	40.051	10,654		5.88	1.03	3.57	6.50	1.28	29.02	8.53	37.46	8.13	0.00	12.65	0.69
FC16-W4	Xb	Gneiss	Fourmile Snowmelt/ 008	5/25/16	−105.568	40.053	11,432		166.22	11.93	38.91	22.46	0.00	72.62	9.42	38.00	12.44	11.56	14.20	17.28

TABLE A2 Use of ^{22}Na as an indicator of transit time

Site	Sample	mg Na extracted	Litres equilibrated wrt Na	Net counts/ksec	Counts/ksec/L	mBq/L	Decay Corrected (mBq ^{22}Na/L)[a]	Estimated mean transport time, in years
Como Creek at MRS	1	151	95.57	0.08981	0.000939	0.055605	0.068824	~2–3
Columbine spring	2	274	72.87	<0.05	0.000686	*0.038118*	*0.042977*	NA
U. Fourmile Cr	3	131	139.36	<0.05	0.000358	*0.015945*	*0.017978*	NA
U. Como Cr.	4	526	367.83	0.17	0.000462	0.027347	0.031246	~4–6[b]
U. Fourmile Cr. at snowfield	5	486	341.05	0.09	0.000185	0.010957	0.012688	~8–10[b]
U. Como Cr. at snowfield	6	670	430.87	<0.05	0.000116	*0.006866*	*0.007845*	NA

[a]Unpublished data from James Kaste, College of William and Mary; values in italics are not significant.

[b]Maximum time based on ^{22}Na activity. Likely 10× too long because of first flush effects.